COMPUTATIONAL INVESTIGATION AND MECHANOCHEMICAL SYNTHESIS OF CROWN ETHER CO-CRYSTALS

Dissertation submitted to the University of Kerala in partial fulfilment of the requirements for the award of the degree of Master of Science in Analytical Chemistry

Subject Code: CL 243

Exam Code: 63620401

MSc. Analytical Chemistry

CONTENTS

ABBREVIATIONS

CCDC	Cambridge Crystallographic Data Centre
CSD	Cambridge Structural Database
DFT	Density Functional Theory
FIMs	Full Interaction Maps
LAG	Liquid-Assisted Grinding
T_m	Melting Temperature
VMD	Visual Molecular Dynamics
18C6	18-Crown-6
DCH18C6	Dicyclohexano-18-crown-6
B18C6	Benzo-18-crown-6
DB18C6	Dibenzo-18-crown-6
POLAG	Polymer Assisted Grinding

ABSTRACT

Computational and experimental research are the two scientific avenues moving concurrently. Here we explore the conformation data analysis of a series of 18C6 and substituted 18C6 using the potential of computational approaches and also mechanochemically prepare the binary and ternary co-crystals of the less-studied DB18C6. Firstly, we sort out the conformations of crown ethers using CONQUEST, MERCURY, VMD, and Gaussview 6.0 from the list of reported co-crystal data. This investigation reveals the impact of conformations on cocrystallization. Secondly, through mechanochemical preparation of binary and ternary system of DB18C6 in the presence of methanol (50 μL) as the liquid phase and using a high-energy micro ball mill, we explored and optimized the efficient formation of the multicomponent systems. The resultant co-crystals were characterized by optical microscopy, hot-stage, and powder X-ray diffraction (PXRD).

CHAPTER 1

INTRODUCTION

Crystal engineering is a rapidly developing area of research that focuses on rationalizing the design of solids[1]. The scope of research is related to the design of solids with predictable properties (e.g., optical, magnetic, reactivity), based on an understanding of factors such as intermolecular forces, molecular sizes, shapes, etc., that influence the molecular assembly in the crystalline state. The beginnings of crystal engineering are primarily attributed to the work of Schmidt, which focused on reactivity in the organic solid-state. It is a natural outcome of the interplay between crystallography and chemistry[2]. Chemistry deals with the study of molecules, whereas crystallography deals with that of crystals, which corresponds to an extended ordered assembly of molecules. The interplay between chemistry and crystallography is, hence, the interplay between the structure and properties of molecules on the one hand and those of extended assemblies of molecules on the other[1]. The inter-relationship between molecules and crystals was first addressed by W. H. Bragg, who recognized that "*Certain structural units like a benzene ring have a definite size and form that might be retained with hardly any change on going from one crystal structure to another*"[1].

In the crystal engineering field, components for co-crystal formation are chosen on the basis of their ability to utilize known intermolecular interactions in forming those crystals. Crystal engineering uses a combination of directional interactions of the molecules to form the crystal's required supramolecular architecture and achieve the desired properties. Co-crystals made from crown ethers are of great interest to the theoretical chemist as they have great potential for effectively designing highly complex, functional molecular solids from simple building blocks. Cyclic polyethers were known long before, and Pedersen was only the first to indicate their outstanding binding properties[3]. Crown ethers, since their discovery, have witnessed immense interest in their chemistry and the physical aspects that find extensive utility in a vast repertoire of applications.

They possess features such as:

(i) structural flexibility, or the tendency of crowns to adopt different conformations under different conditions;

(ii) cation specificity, or the preference (significant interaction free energy or enthalpy) of the crown for certain cations; and

(iii) the macrocyclic effect, or the incredible binding free energy of the ligand to crowns than to open-chain analogs.

Hence, they are helpful in various fields such as cancer treatment, nuclear waste treatment, catalysis, control of reaction mechanisms, second-sphere coordination, ion transport, etc. Because of the widespread applications of crown ethers, there has been a great interest in their conformational analysis.

Our present work focuses on studying various conformations of the crown ether series such as 18C6, DCH18C6, B18C6, and DB18C6 with neutral molecules, computationally, in parallel with experimental work on the preparation of binary and ternary co-crystals of DB18C6.

1.1 COMPUTATIONAL CHEMISTRY

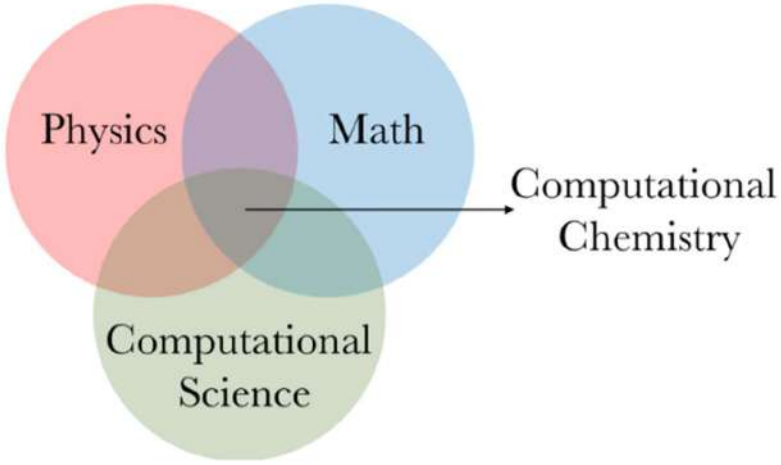

Fig.1.1: Computational chemistry (Adapted from Ref.4)

Computational chemistry is a rapidly emerging subfield of theoretical chemistry, where the primary focus is solving chemically related problems by calculations. Computational methods in chemistry are a subject that is interdisciplinary and brings together physics, chemistry, mathematics, and computer science, all under one umbrella (Fig.1.1). It uses computer simulation to assist in solving chemical problems, and the methods of theoretical chemistry were incorporated into computer programs to calculate the structures and properties of molecules, groups of molecules, and solids. A new field of computational chemistry was born in the late 1990s when Walter Kohn and John Pople formulated computational methods

in quantum chemistry through their work on DFT[4]. Mathematical and computational algorithms, statistics, and large databases are used to combine DFT with experimental measurements[5]. Some exploration areas addressed by computational chemistry are (1) Reactivity modeling (2) Fundamental physical processes behind phenomena such as charge storage, pseudo capacitance, corrosion, phase changes, etc. (3) Modelling a complex system consisting of hundreds of atoms, molecules, and ions. Some tools are electronic structure methods, molecular dynamics, and cluster calculations. It is widely used in the design of new drugs and materials. Our study used these methodologies to determine the energies of various conformations of crown ether series.

1.1.1 CONFORMATIONS OF CROWN ETHERS:

Crown ethers are defined as the macrocyclic oligomers of ethylene oxide in the form of $(–CH_2CH_2O–)$ n with $n \geq 4$. The oxygen atoms in crown ethers are well situated to coordinate with cations located in the interior of the macrocyclic polyethers, whereas the exterior of the macrocycles is hydrophobic, which renders the complexed cation soluble in organic solvents[3]. The crown ethers are usually represented by [m]crown-'n', where 'm' represents the total number of atoms "in the macrocycle, and 'n' represents the number of oxygen atoms in the macrocycle.

Macrocyclic crown ethers are well-known molecules in host-guest chemistry. The importance of these ethers originates from their remarkable selectivity in the encapsulation of guest species. Efficient capture of a guest species can easily be achieved by using suitable ethers whose cavity size is similar to that of the guest. For example, [18] crown-6 (Fig.1.2) has a high affinity for K^+, [15]crown-5 for Na^+, and [12]crown-4 for Li^+ ions.[3] On the other hand, crown ethers change their conformations and adjust the size and anisotropy of the cavity to accept various kinds of guests. In addition, conformations of crown ethers are highly affected by their environment. The efficiency of molecular binding is also determined by the structure of the binding sites in the crown ether cycle. V. P. Barannikov *et al.* from their studies, found that, with the same charge distribution over the atoms in a series of crown ethers having different sizes of the cycle, from 12-crown-4 to 21-crown-7, the most stable are the complexes of 18-membered cycles[6]. The molecular flexibility and the distances between the six binding sites in the 18C6 molecule create the most favorable conditions for structural compliance for specific interactions with the majority of molecules.

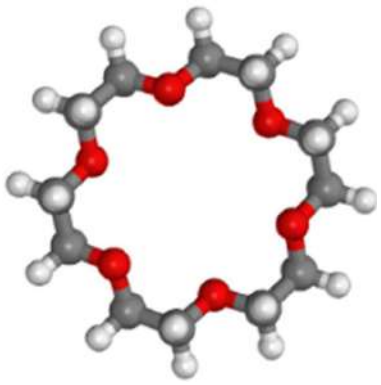

Fig.1.2: [18] crown-6

Conformational analysis of the 18C6 series was mainly studied on its complexes with Group IA, Group II A, charged molecules, and ions. Stable conformations of the 18C6 with alkali metal complexes are mainly attributed due to the maximum attraction between the cation and the lone pairs of the oxygens and minimum repulsion between lone pairs. This is achieved with backbone structures of crown ethers that are open for the larger cations, Cs^+ and K^+(Fig.1.3), and folded for the smaller cations, Na^+ and Li^+. The flexibility of the crown ether backbone, cavity size, and symmetry constraints are of key relevance in the stability of these complexes.

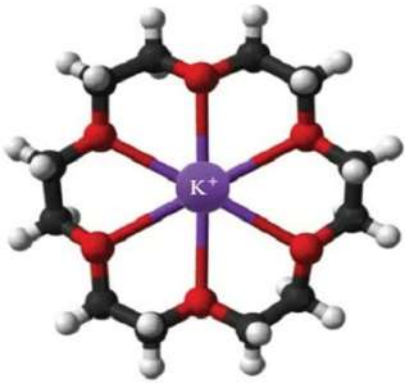

Fig.1.3: 18C6 complex with K^+.

Recently, studies have shown the complex formation of the 18C6 series with neutral molecules. The stability of these complexes is mainly attributed to non-covalent and weak van der Waals interactions such as hydrogen and halogen bond interaction. Since hydrogen bonds are among the strongest, preferential and directional intermolecular interactions, they have been the leading element for the interactions to be utilized in forming co-crystals. The

complexation of crown ether series with neutral molecules led us to study the conformations adopted by crown ether in various complexes.

1.2 MECHANOCHEMISTRY AND COCRYSTALLIZATION

'Mechanochemistry' is defined as a chemical synthesis method, mainly solids, by inducing chemical and physicochemical transformations through mechanical force generated by grinding and milling[7]. The history of mechanochemistry is quite old, with first reports dating back to the 4th century BC, when cinnabar was reduced by grinding in a copper vessel in the presence of vinegar, extracting elemental Hg[8]. It has gained paramount interest as a powerful, more sustainable, timesaving, environmentally friendly, and more economical synthesis method to prepare developing functional materials. Thus finds an increased development in generating complex organic molecules, multicomponent organic solids (co-crystals, salts, solvates, and hydrates), supramolecular assemblies, metal-organic framework, and the development of novel solid forms of active pharmaceutical substances and their testing. It has paved a new way for producing co-crystals, potentially impacting the pharmaceutical industry. Co-crystal is "*A solid that is crystalline materials composed of two or more molecules in the same crystal lattice*".[9] Applications of co-crystals range from advanced pharmaceutical materials, molecular semiconductors, and optical materials to media for stereo-controlled synthesis[10]. Co-crystals are continuously being expanded with halogen and hydrogen-bonding functional groups and supramolecular synthons, expanding the diversity of potential co-crystals and co-crystal components.

Co-crystals are often prepared by traditional solution cocrystallization approaches such as solvent evaporation, vapor or solvent diffusion, antisolvent addition, or cooling. An effective alternative approach for co-crystal synthesis is solid-state grinding or neat (dry) grinding (NG) and liquid-assisted grinding (LAG). In the solid-state grinding technique, two solids are ground together either manually, using a mortar and pestle, or mechanically, using a ball mill (Fig.1.4: a) and b)). Milling can be carried out in a variety of ways. The simplest is the laboratory mortar and pestle. This hand milling method can produce many mechanochemical reactions that do not necessitate overcoming a high energy barrier. When higher energy is required ball mills are used.

a) b)

Fig.1.4: a) Mortar and pestle and b) Micro ball mill

Mechanochemical reactions are affected by various factors such as nature[11] or amount of liquid additives used during grinding, nature of milling, materials used in grinding jars and balls[12], milling frequency[13], medium to sample weight ratio[14], etc.

A major enhancement to this method was recently achieved by adding a few drops of solvent to the grinding mixture, termed liquid-assisted grinding (LAG). The method was originally termed "*solvent-drop grinding*",[10] but this name is no longer preferred, primarily reflecting different ideas concerning the mechanism in the presence of the liquid. It evolved from kneading, wherein a small amount of a liquid, measured by the ratio of liquid volume to reactant weight (η) is introduced into a milling jar along with reactants and milling ball[15]. In LAG, the liquid medium accelerates the reactions that do not proceed by neat milling. Parameter η is used to characterize LAG reactions and compare them to other methods. A value of $\eta = 0$ corresponds to neat grinding, $\eta > 10$ μL/mg corresponds to a typical solution reaction[16]. Systematic study of cocrystallization by milling led to an empirical definition of LAG as the η range of ca. 0-2 μL/mg, where reactant solubility does not affect reaction outcome[15]. At higher η (in slurry or solution), cocrystallization becomes hindered or prevented by incongruent solubility of reactants.

1.2.1 BINARY AND TERNARY CO-CRYSTALS

Cocrystallization is the process of producing co-crystals, where more than one organic compound is induced into the same crystal lattice. Co-crystals are essential as they provide a route to the controlled modulation of crystal properties. The Heterosynthon concept flagged

the way to co-crystal synthesis, which considers the complementary recognition of chemical groups from different molecules, such as lock-and-key, bumps-in-hollows, donor−acceptor interactions[17], hydrogen bonds, and halogen bonds[18,19]. Halogen bonding has elicited much recent interest in the context of crystal engineering. The halogen bond is similar to a hydrogen bond in that the halogen atom is electrophilic. It has adequate strength and directionality to constitute an excellent middle ground between strong and weak hydrogen bonds in the overall hierarchy of intermolecular interactions. Recently, several studies have used halogen bonding along with hydrogen bonding in the design of binary co-crystals. A graded and sequential approach to interaction selection will allow for the designed synthesis of a ternary co-crystal whose architecture is purely interaction-based. Halogen bonds are of suitable strength and directionality and may be used along with hydrogen bonds in the crystal engineering of complex targets. This concept of hydrogen and halogen bond interactions can be applied to the synthesis of binary and ternary co-crystal of DB18C6.

CHAPTER 2

LITERATURE REVIEW

Crown ethers, which are significant because of their exceptional selectivity in encapsulating guest species, can modify their conformations and adjust the cavity's size and anisotropy to accommodate diverse types of guests. Furthermore, the environment and substituents on it significantly impact crown ether conformations.

In 1979, Johannes Dale studied various conformations of free and complexed oligo ethers using X ray and ^{13}C NMR. The 1,4,7,10,13,16-Hexaoxacyclooctadecane (18-crown-6), in its complexes with a variety of cations, adopts a centrosymmetric non-angular D_{3d} conformation[20].

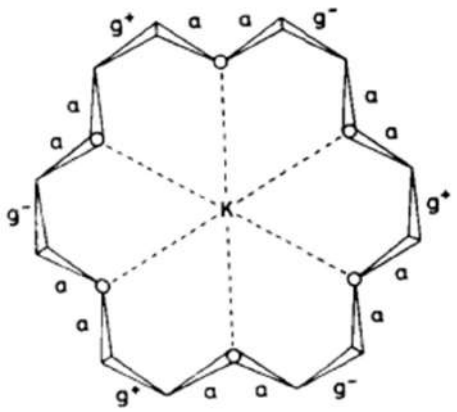

Fig.2.1: (a) Crystal structure of 18crown6 with KSCN (1:1)

A conformational study of the structure of free 18-Crown-6 by Azhary and co-workers in 2005 used the CONLEX method at the MM3 level. To have a more accurate energy order of the predicted conformations, the predicted conformations were geometry optimized at the HF/STO-3G level, at the HF/6-31+G* level, and hereafter at the B3LYP/6-31+G* level. They found that, at the MP2/6-31+G*//B3LYP/6-31+G* level, there are three conformations that have energy lower energy than C_i, and the S_6 with the lowest energy conformation is more stable than the experimentally known C_i confirmation by 1.96 kcal/mol[21].

Molecular dynamics study of the structure and dynamics of the 18-crown-6 in a vacuum and in cyclohexane by F. T. H. Leuwerink and W. J. Briels using the simulation package GROMOS, made an extensive comparison of the structural characteristics of the crown ether

molecule in both cases. They observed that conformational statistics were almost the same in vacuo and the apolar cyclohexane. However, the structure of the crown ether is found to fluctuate around the centrosymmetric C_i conformation[22].

Peter Kollman et al. studied different conformations of 18-crown-6 and its alkali-cation complexes[23]. The lowest-energy conformers for the crown and its complexes were observed by X-ray crystallography. With a low dielectric constant for the crown itself, they calculate that the lowest-energy structure is of C_i symmetry. However, D_{3d} structure becomes of similar energy in a more polar environment. They also predicted the existence of C_1 symmetry. They observed that the lowest-energy conformation of the Na^+/crown structure is of the type C_1, and for K^+/crown it is D_{3d} type; both are observed in the solid-state.

a) b)

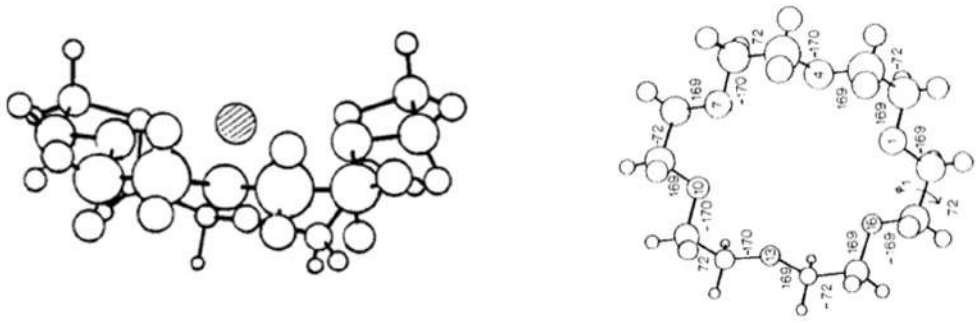

Fig.2.2: (a) The optimized structure for Na+-crown complex (C_1) (b)Energy optimized D_{3d} structure.

G. Bombieri *et al*. studied the crystal and molecular structure of $Nd(NO_3)_3$(18-Crown-6) and highlighted that the crown ether displays pseudo C_2 symmetry: a twofold axis perpendicular to the plane of the etheric oxygens and bisecting a nitrate group crosses the molecule[24].

Takakiarai, *et al*, studied the structure of 18-crown-6 and their metal complexes in methanol solution by Raman spectroscopy. Raman spectra of 18-crown-6 and it's complexes with Li^+, Na^+, K^+,Cs^+, Mg^{2+}, Ca^{2+} and Ba^{2+}were investigated in methanol solution. Raman spectra analysis found that the uncomplexed ethers adopt diverse conformational states in methanol at room temperature, where C_i form is stable only in crystal, is not populated significantly in solution, and the D_{3d} state is the most stable in 18-crown-6[25].

a) b)

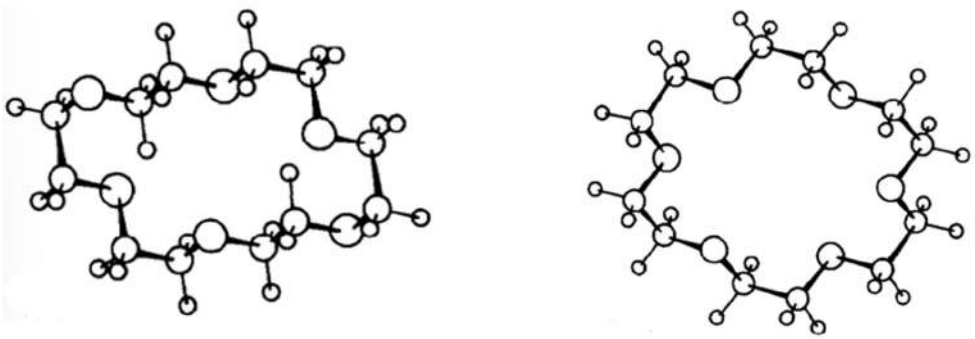

Fig.2.3: Conformers of 18-crown-6 with C_i and D_{3d} symmetry.

N. Kent Dalley*et al* determined the crystal structure of the barium-complex of isomer A of the cyclic poly-ether dicyclohexyl-18-crown-6 by X-ray diffraction: the isomer A is in the cis-syn-cis-conformation. Crystal data shows that the poly-ether molecule possesses C_2 symmetry, and the barium atom lies on the two-fold axis[26], shown in Fig below.

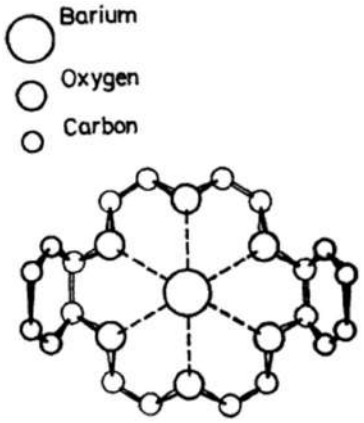

Fig.2.4: Dicyclohexy-l8-crown-6 (isomer A) complex

A. Navaza and F. Villain studied the crystal structure of Dicyclohexyl-(18-crown -6) uranyl perchlorate (Complex I) and Dicyclohexyl (18-crown -6) uranyl hydroxy-perchlorate acetonitrile (Complex II), through three-dimension X-ray diffraction data and determined that in Complex I crown ether shows *cis-anti-cis* conformation (Fig.2.5(a)) and in Complex II crown ether shows two conformations (i) *cis-anti-cis* and (ii) *cis-syn-cis* conformations[27] (Fig.2.5(b)).

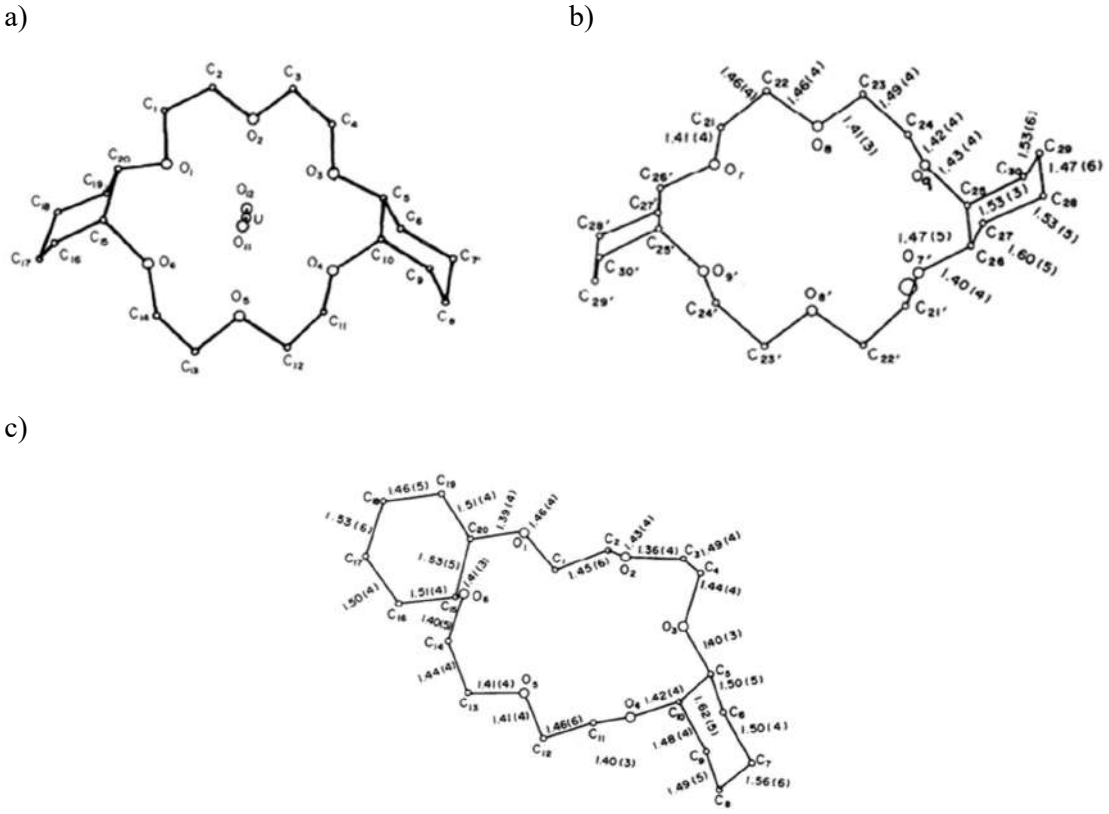

Fig.2.5: (a) cis-anti-cis conformation of dcc in Complex I.(b); (i) cis-anti-cis conformation of dcc in Complex II. Fig. (b); (ii) cis-syn-cis conformation of dcc in Complex II.

Ryoji Kusaka, Yoshiya Inokuchi, and Takayuki Ebata carried out a laser spectroscopic study on the conformations and the hydrated structures of benzo-18-crown-6-ether and dibenzo-18-crown-6-ether in supersonic jets[28]. They applied laser-induced fluorescence (LIF) spectroscopy, UV-UV hole-burning spectroscopy, and IR-UV double-resonance spectroscopy to jet-cooled B18C6 and DB18C6. In parallel, they also performed a quantum chemical calculation to obtain probable structures and their IR spectra. Geometry optimization and vibrational analysis at the B3LYP/6-31+G* level of theory using GAUSSIAN 03 posited four conformers possible for bare B18C6 and three for B18C6-$(H_2O)_1$. The proposed four conformers of B18C6 are C_2, C_2 trans, D_{3d}, and deformed D_{3d} (Fig.2.6).

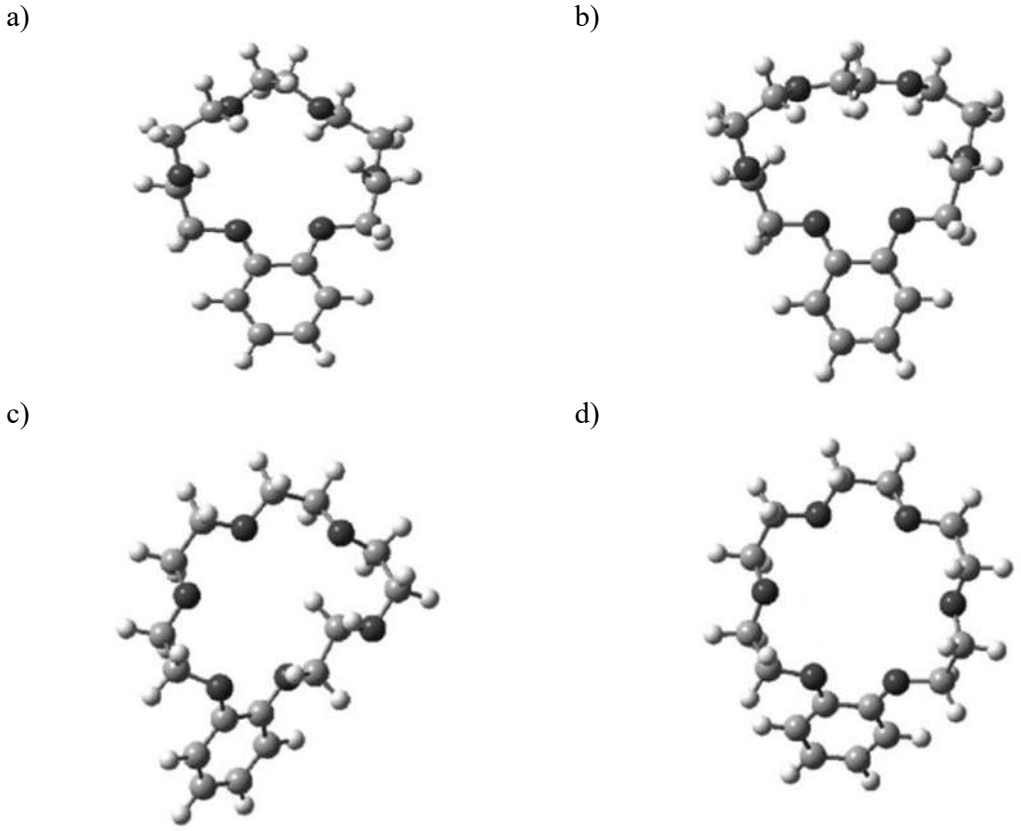

Fig.2.6: Optimized structures of the B18C6 monomer at the B3LYP/6-31+G* level of theory (a) C_2(b) C_2trans (c) Deformed D_{3d} (d) D_{3d}

Two stable conformers are possible for DB18C6 and a single conformer for DB18C6 $(H_2O)_1$. The lowest energy conformer of DB18C6 has a C_{2v} structure, called the "boat" type. The second one has a "chair" type structure and a C_i symmetry. (Fig.2.7)

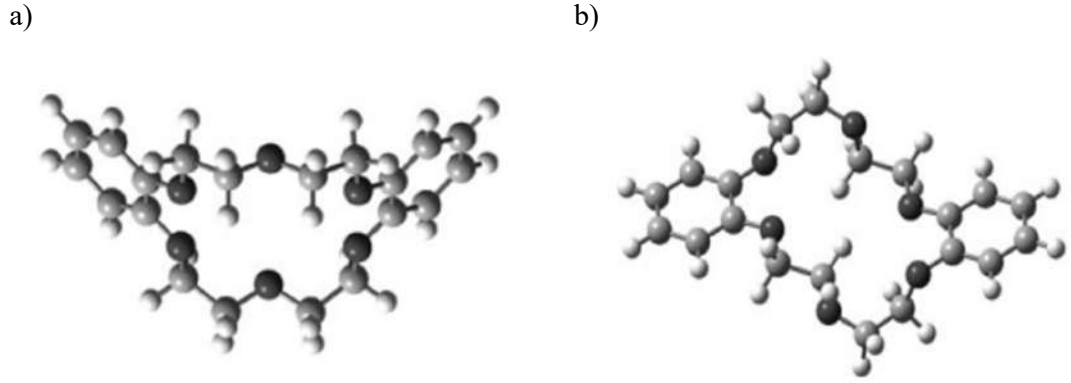

Fig.2.7: Optimized structures of the DB18C6 monomer and the DB18C6-$(H2O)_1$ at the B3LYP/6-31+G* level of theory. (a) Boat conformation (b) Chair conformation

Crown ethers, because of their multiple non-covalent interactions with complimentary guest cations, has been extensively used in supramolecular chemistry and crystal engineering for various cationic species, creating a variety of molecularly assembled structures. There are many studies regarding the binary and ternary co-crystal formation by18C6 ether series.

Gerrit J Van Hummel *et al.* studied the crystal structure of 18crown6 with urea (1:5) complex. A molecular complex of urea and 18-crown-6 (5:1) was prepared by the addition of diethyl ether to a homogeneous solution of 264 mg of 18-crown-6 and 90mg of urea in methanol-chloroform (1:2). Recrystallization from methanol-ethyl acetate yielded the analytically pure 5: 1 complex. The crystal structure of the complex was determined by X-ray crystallography. The urea 18-crown-6 complex described here represents the first example of the structure determination of a urea molecule bonded to a macrocyclic ether. The results also demonstrate the potential importance of hydrogen bonds in the design of synthetic receptors for urea-like molecules[29].

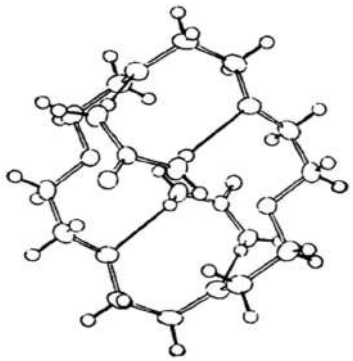

Fig.2.8: Hydrogen bonds between 18crown6 and urea molecules.

Michael G B Drew *et al.* studied the structure of 1:2 adduct of 18crown6 with thiourea. The 1:2 adduct was prepared by dissolving thiourea (0.76 g) in hot methanol (10 ml) and adding a hot solution of 18-crown-6 (2.64g) in methanol (10 ml). Crystals formed were analysed by X-Ray crystallography, with intermolecular hydrogen bonding being the particular interest of the study[30].

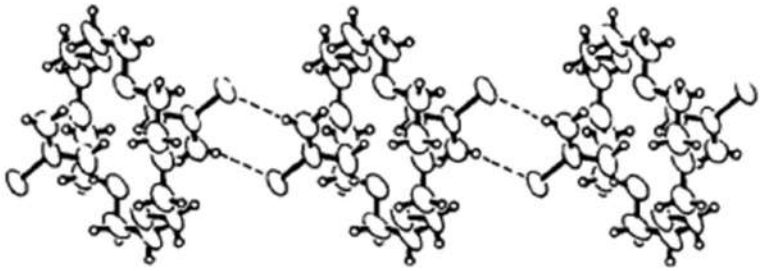

Fig.2.9: The packing of the 18-crown-6-thiourea (1:2) adduct along the y axis. The N-H...S intermolecular hydrogen bonds are shown as dashed lines.

Filip Topić and Kari Rissanen, 2016, displayed a carefully planned technique for constructing ternary co-crystals based on the orthogonality of two supramolecular interaction modes: hydrogen bonding between crown ethers and thioureas and the halogen bonding between thioureas and perfluorohalocarbons[31]. They tested on a set comprising two crown ethers (18C6, B18C6), two thioureas (thiourea and methyl-substituted thiourea), and five halogen bond donors; the crystals formed were analyzed by X-ray crystallography. The technique resulted in a 75% success rate, with 15/20 component combinations yielding at least one co-crystal.

Elena A. Chulanova, NikolayA. Semenov *et al*, studied the molecular complexes formed by the cocrystallisation of 1,2,5-chalcogenadiazoles (chalcogen E = S, Se, and Te) with cyclic polyethers 18-crown-6 (18C6) and dibenzo-18-crown-6 (DB18C6). Molecular complexes formed were characterized by X-ray diffraction and thermogravimetry/differential scanning calorimetry techniques, DFT calculations, and quantum theory of atoms in molecule and natural bond orbitals analysis. The complexes are bound by multiple secondary bonding interactions, the most important of which reflects the Lewis amphiphilicity of 1,2,5-chalcogenadiazoles, chalcogen bonding (ChB), i.e., the attractive interactions between chalcogen sites in molecules and Lewis bases/nucleophiles, which is a kind of secondary bonding interaction, includes charge transfer from O atoms of the ethers onto E atoms of the chalcogenadiazoles (i.e., chalcogen bonding), and the back-donation from E to O[32].

a) b)

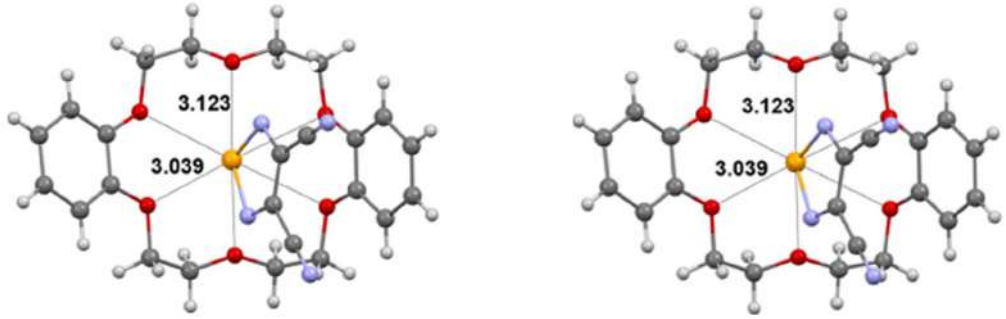

Fig.2.10: Dotted line indicates chalcogen bonding between a) sulphur b) selenium with DB18C6

The present work highlights a strategy for studying various conformations of crown ether series (18C6, DCH18C6, B18C6, DB18C6) in binary and ternary systems. From CCDC data, it is observed that D_{3d}, C_i, C_1, and C_{2v} are the major conformations of 18C6, DCH18C6, B18C6, and DB18C6, respectively. Energy optimization and energy for the various conformations are calculated using Gaussian6.0. Relative energies are calculated, thereby predicting the most stable conformation. A full interaction map is studied to understand the possible interactions of various conformations of crown ether series. Knowledge of the non-covalent interactions such as hydrogen and halogen bonding is utilized for preparing binary and ternary co-crystals of DB18C6.

SCOPE AND OBJECTIVES OF THE STUDY

1. Analysis of various conformations of crown ether series computationally.
2. Calculating the energy of various conformations using Gauss View 6.0
3. Full interaction maps (FIMs) studies of various conformations.
4. Preparation of binary and ternary co-crystals in the ratio 1:2 and 1:2:2 respectively, using the principles of mechanochemistry.
5. Recrystallisation of both binary and ternary co-crystal by solvent evaporation method.
6. Characterisation of co-crystals by following techniques:
   - Melting point determination by hot-stage and optical microscope.
   - PXRD analysis.

CHAPTER 3

MATERIALS AND METHODS

3.1 MATERIALS:

All reagents and solvents used for the co-crystal formation were purchased from commercial sources. The chemicals and solvents were used without any further purification.

3.2 METHODS:

3.2.1 Computational methods used:

Using CCDC, complexes of 18C6 series with neutral molecules are determined. Various conformations of 18C6 ether series are studied using VMD. Mercury is used for FIMs analysis. Energies of various conformations are calculated using Gaussian 16W at the B3LYP/6-311++G(d,p) level, where all bonds to H atoms are normalized. The relative energy (ΔE) is calculated as the difference between the optimized energy and total energy.

Computational chemistry is a branch of chemistry that uses computer simulation to assist in solving complex chemical problems. It exploits methods of theoretical chemistry, incorporated into efficient computer programs, to calculate the structures, the interactions, and the properties of molecules[34]. Computational chemistry numerically simulates chemical structures and reactions based in full or in part on the fundamental laws of physics. It allows chemists to study chemical phenomena *in silico* rather than by examining reactions and compounds experimentally. Some methods can be used to model not only stable molecules but also short-lived, unstable intermediates and transition states. In this way, they can provide information about molecules and reactions, which is impossible to obtain through observation.

BASIS SET:

A basis set in computational chemistry is a set of functions called basis functions, which are combined in linear combinations, generally as part of a quantum chemical calculation, to create molecular orbitals. For convenience, these functions are typically atomic orbitals centered on atoms but can theoretically be any function; plane waves are frequently used in materials calculations.

SLATER TYPE ORBITALS

In the early days of quantum chemistry, the so-called Slater-type orbitals (STOs) are used as basis functions due to their similarity with the eigenfunctions of the hydrogen atom. This type of orbitals gives a better approximation, in which the nuclear charge that appears is used as a variational parameter that accounts for the shielding effects due to electron-electron interactions. Using atomic orbitals allows us to interpret molecular properties and charge distributions in terms of atomic properties and charges, giving the picture that molecules are composed of atoms.

STOs have the following radial part (the spherical harmonic functions are used to describe the angular part)

$$R(r)=Nr^{n-1}\ e^{-\zeta r}$$

Where 'n'is a natural number that plays the role of a principal quantum number, n = 1, 2..., 'N' is a normalizing constant, 'r"" is the distance of the electron from the atomic nucleus, and 'ζ' is a constant related to the effective charge of the nucleus, the nuclear charge being partly shielded by electrons.

DOUBLE-ZETA BASIS SET

One can use more than one STO to represent one atomic orbital. The linear combination of the function describes the charge distribution in the molecule (for the ground state). The function with the large zeta accounts for a charge near the nucleus, while the smaller zeta accounts for the charge distribution at larger values of the distance from the nucleus. This expanded basis set is called a double-zeta basis set. It can be represented as

$$R_{2s}(r)=C_1re^{-\zeta_1 r}+C_2re^{-\zeta_2 r}$$

where C_1 and C_2 are coefficients

GAUSSIAN ORBITALS

The use of complex integrals led computational chemists to seek alternatives. As a result, Slater-type orbitals were replaced by Gaussian expansions in molecular calculations. The computation of the integrals is greatly simplified by using Gaussian-type orbitals (GTO) for basic functions[33]. It is given by;

$$G_{nlm}(r,\theta,\Psi) = N_n r^{n-1} e^{-\alpha r^2} y_l^m(\theta,\Psi)$$

Unfortunately, Gaussian functions do not match the shape of an atomic orbital very well. In particular, they are flat rather than steep near the atomic nucleus at r=0, and they fall off more rapidly at large values of r.

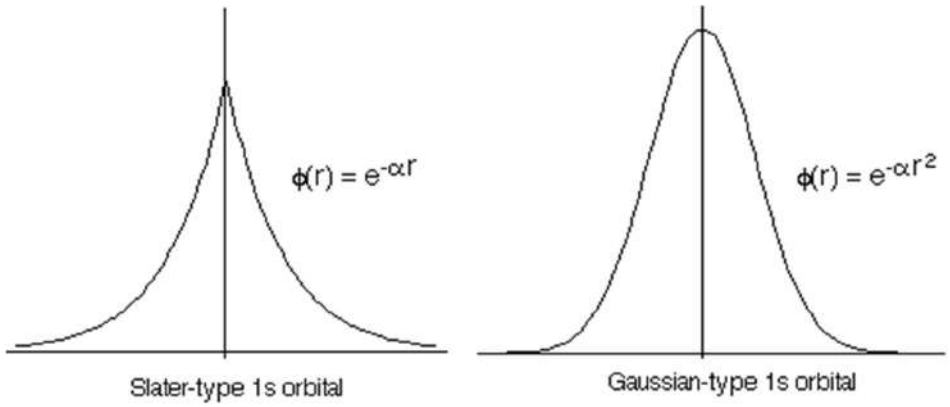

Fig.3.1: Radial Dependence of Slater and Gaussian Basis Functions. Image used with permission.

To compensate for this problem, each STO is replaced with a number of Gaussian functions with different values for the exponential parameter. These Gaussian functions form a primitive Gaussian basis set. Linear combinations of the primitive Gaussians are formed to approximate the radial part of an STO. This linear combination is not optimized further in the variational energy calculation but rather is frozen and treated as a single function. The linear combination of primitive Gaussian functions is called a contracted Gaussian function. Although more functions and more integrals now are part of the calculation, the integrals involving Gaussian functions are quicker to compute than those involving exponentials, so there is a net gain in the efficiency of the calculation.

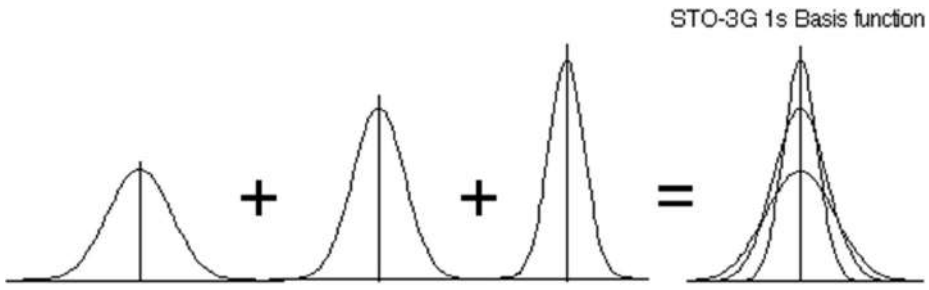

Fig.3.2: GTO basis sets are constructed from fixed linear combinations of Gaussian functions, and contracted GTOs (CGTO).

Gaussian basis sets are identified by abbreviations such as N-MPG*. N is the number of Gaussian primitives used for each inner-shell orbital. The hyphen indicates a split-basis set

where the valence orbitals are double zeta. The M indicates the number of primitives that form the large zeta function (for the inner valence region), and P indicates the number that forms the small zeta function (for the outer valence region). G identifies the set as being Gaussian.

Basis sets approximate orbitals by assigning a group of basis functions to each atom within a molecule. Each basis function is composed of a linear combination of Gaussian functions, referred to as Contracted functions, and the Gaussian component functions are referred to as Primitives. The uncontracted basis function consists of only one single Gaussian function. More extensive basis sets approximate the orbitals more accurately by imposing fewer restrictions on the location of electrons in space. An individual molecular orbital is defined as:

$$\phi_i = \sum_{\mu=1}^{n} c_{\mu i} x_\mu$$

Basis sets are classified into five types, minimal basis set, split valence basis set, polarised or Pople basis set, diffused basis set, and correlation-consistent basis sets. A minimal basis set contains a minimum number of basis functions to describe each atom. It selects one basis function for every atomic orbital required to describe the free atom. The form STO-kG is considered to be a minimal basis set. In the Split valence basis set, an additional basis function, one contracted Gaussian plus some other primitive Gaussian functions, is assigned to describe the valence orbital. These basis sets are characterized by a number of functions assigned to the valence orbital.3-21G and 6-31G are considered to be split valence basis sets. Polarised or Pople basis set add orbitals with angular momentum going beyond of requirement for the description of the ground state of each atom at the HF level.6-31G(d), 6-311G(d,p) are considered to be polarised or Pople basis set. Diffused basis set describes the electron density away from the nucleus. They are indicated by a + symbol in the notation.6-31+G is 6-31G plus diffuse s and p functions for nonhydrogen atoms; 6-31++G has diffuse functions for hydrogen. Correlation-consistent basis sets have the unique property of forming a systematically convergent set. Calculations using this basis set give accurate estimates of the Complete Basis Set (CBS) limit. Represented by cc-pVnZ

There are two broad areas within computational chemistry devoted to the structure of molecules and their reactivity: molecular mechanics and electronic structure theory. They perform the same basic types of calculations:

1. Computing the energy of a particular molecular structure. Properties related to the energy may also be predicted by some methods.
2. Performing geometry optimizations, which are an attempt to locate the lowest energy molecular conformation.
3. Computing the vibrational frequencies of molecules resulting from interatomic motion within the molecule.

MOLECULAR MECHANICS:

Molecular mechanics simulations use the laws of classical physics to predict the structures and properties of molecules. They are many different molecular mechanics methods. Each one is characterized by a force field. A force field has the following components:

1. A set of equations defines how a molecule's potential energy varies with the locations of its component atoms.

2. A series of atom types defines an element's characteristics within a specific chemical context. The atom type prescribes different characteristics and behavior for an element depending upon its environment. The atom type depends on hybridization, charge, and the types of the other atoms to which an atom is bonded.

3. One or more parameter sets fit the equations and atom types to experimental data. Parameter sets define force constants, which are values used in the equations to relate atomic characteristics to energy components, and structural data such as bond lengths.

Molecular mechanics calculations do not explicitly treat the electrons in a molecular system. Instead, they perform computations based upon the interactions among nuclei. Electronic effects are implicitly included in force fields via their parametrization.

This approximation makes molecular mechanics computations relatively inexpensive in computation time and allows them to be used for extensive systems containing thousands of atoms. However, it also carries several limitations:

1. Particular force fields achieve good results only for a limited class of molecules related to those for which it was parametrized. No force field can be generally used for all molecular systems.

2. Neglect of electrons means that molecular mechanics methods cannot treat chemical problems where electronic effects predominate.

ELECTRONIC STRUCTURE METHODS:

Electronic structure methods use the laws of quantum mechanics rather than classical physics as the basis for their computations. Quantum mechanics states that the energy and other related properties of a molecule may be obtained by solving the Schrödinger equation:

$$H\Psi = E\Psi$$

For any but the smallest, totally symmetric systems, however, exact solutions to the Schrödinger equation are not practical. Electronic structure methods are characterized by their various mathematical approximations to their solution. There are two major classes of electronic structure methods:

AB INITIO METHOD:

Unlike either molecular mechanics or semiempirical methods, these methods use no experimental parameters in their computations. Instead, their computations are based solely on the laws of quantum mechanics —the first principles referred to in the name ab initio— and on the values of a small number of physical constants: The speed of light, the masses, and charges of electrons and nuclei, Plank's constant. Equation proves intractable when trying to find exact solutions for chemical systems larger than a hydrogen-like atom. Methods such as Hartree-Fock (HF), Møller-Plesset (MP), coupled-cluster (CC), and configuration interaction (CI) approaches have been developed to approximate the solution to the Schrödinger equation. Ab Initio methods are also often referred to as "Electronic Structure Methods" as they rely on solving the electronic state of the system, that pertaining to the electrons, to calculate various properties of the system. The most common type of ab-initio calculation is called Hartree-Fock calculation (abbreviated HF), in which the primary approximation is called the mean-field approximation.

Hartree–Fock (HF) method is a method of approximation for the determination of the wave function and the energy of a quantum many-body system in a stationary state. The Hartree–Fock method is also called the self-consistent field method (SCF). In the self-consistent field Hartree-Fock (SCF-HF) method, the variational principle is applied with a single Slater determinant to obtain approximated ground state wave functions and their eigenvalues, that is, energies.

The Hartree-Fock differential equation has the form:

$$F(1)\Psi i = E_i\Psi_i(1)$$

Where Ψ_i is the i^{th} spin-orbital, E_i is the corresponding energy.

The Fock operator (F) is defined as follows:

$$F(1) \equiv -\frac{1}{2}\nabla_1^2 - \sum_{\alpha}\frac{z_\alpha}{r_1\alpha} + \sum_{j=1}\left[J_j(1) - k_j(1)\right]$$

SEMIEMPIRICAL METHOD:

Semiempirical Methods are simplified versions of Hartree-Fock theory that uses parameter derived from experimental data to simplify the computation. They solve an approximate form of the Schrödinger equation that depends on having appropriate parameters available for the type of chemical system in question. In this method, only a minimal set of valence orbitals are considered on each atom (e.g., 2s, $2p_x$, $2p_y$, $2p_z$ on carbon). Since they do not change much during chemical reactions, core orbitals are not treated by semi-empirical methods. The central assumption of semiempirical methods is the Zero Differential Overlap (ZDO) approximation, in which all products of basis functions that depend on the same electron coordinates located on different atoms are neglected.

DENSITY FUNCTIONAL THEORY:

Density Functional Theory (DFT) is a computational method that derives properties of the molecule based on a determination of the electron density "ρ" of the molecule. Unlike the wavefunction, which is not a physical reality but a mathematical construct, electron density is a physical characteristic of all molecules. DFT is called a functional theory as the energy is a function of the density, E[ρ], which in turn is a function of the position, ρ(r). A functional is a function of a function. Although density functional theory has its roots in the Thomas–Fermi model for the electronic structure of materials, DFT was first put on a firm theoretical footing by Walter Kohn and Pierre Hohenberg in the framework of the two Hohenberg–Kohn theorems (H–K). The H–K theorem was further developed by Walter Kohn and Lu Jeu Sham to produce Kohn–Sham DFT (KS DFT).

First Theorem (Hohenberg and Kohn, 1964): It establishes that the electronic density for a non-degenerate ground electronic state of a molecular system determines the wave function and energy of the ground state and any exited state of the system. It demonstrates one-

to-one mapping between the ground-state electron density with the ground state wave function of a many-particle system. The exact ground state energy (ε_0) can be written as a function.:

$$\varepsilon[\rho_0] = \varepsilon_0 = T_e[\rho_0] + V_{ee}[\rho_0] + V_{eN}[\rho_0] + V_{NN}$$

The second H–K theorem defines an energy functional for the system and proves that the correct ground-state electron density minimizes this energy function. It says that any trial electron density function will give energy higher than (or equal to, if it were exactly the true electron density function) the true ground state energy. In DFT molecular calculations, the electronic energy from a trial electron density is the energy of the electrons moving under the potential of the atomic nuclei. This nuclear potential is called the "external potential", presumably because the nuclei are "external" if we concentrate on the electrons. This nuclear potential is designated v(r), and the electronic energy is denoted by $E_v = E_v[\rho_0]$ (meaning "the E_v functional of the ground state electron density"). The second theorem can thus be stated

$$E_v[\rho_t] \geq E_0[\rho_0]$$

Where ρ_t is the trial electron density, $E_0[\rho_0]$ is the true ground state energy corresponding to the true electronic density $[\rho_0]$.

There are roughly three types, or categories, of density functional methods:

Local density approximation (LDA) methods assume that the density of the molecule is uniform throughout the molecule and is typically not a very popular or useful method. Gradient corrected (GC) methods look to account for the non-uniformity of the electron density. Hybrid methods, as the name suggests, attempt to incorporate some of the more useful features from ab initio methods (specifically Hartree-Fock methods) with some of the improvements of DFT mathematics. Hybrid methods, such as B3LYP, tend to be the most commonly used methods for computational chemistry practitioners.

3.2.2 EXPERIMENTAL METHODS

PREPARATION OF CO-CRYSTALS:

I. preparation of binary co-crystals:

Mechanochemistry is used for the preparation of binary co-crystals of DB18C6 with thiourea and dithiooxamide. Methanol was added as the liquid (LAG) to the reaction mixture.

The mixture was grinded for half an hour using motar and pestle. Recrystallisation was done using suitable solvent systems.

a) Preparation of DBTU:

DB18C6 (50mg, 0.1387mmol) and thiourea (TU, 21.1206mg, 0.2774mmol) i.e., in the ratio 1:2, were grinded with methanol (50µL) as added liquid (LAG) for half an hour. Recrystallization was done using methanol as a solvent system. After two or three days, the formed crystals were collected and analyzed by hot-stage microscopy.

b) Preparation of DBDT:

DB18C6 (74.95mg, 0.2079mmol) and dithiooxamide (DT, 50mg, 0.4159mmol) i.e., in the ratio 1:2, were grinded with methanol (50µL) as added liquid (LAG) for half an hour. Recrystallization was done using methanol as a solvent system. After two or three days, the formed crystals were collected and analyzed by hot-stage microscopy.

II. preparation of ternary co-crystals:

Ternary co-crystals were prepared from the binary mixture (DBTU, DBDT), with halogen donors such as Octafluoro-1,4-diiodobutane (OF), Nonafluoro-1-iodobutane (NF), 1,4-Diiodotetrafluorobenzene (IF) and 1,4-Dibromotetrafluorobenzene (BF), in the ratio 1:2:2.

Ternary co-crystals were prepared from the binary mixture DBTU, with halogen donors such as OF (50.89µL, 0.2774mmol), NF (47.75 µL, 0.2774mmol), IF (111.5048mg, 0.2774mmol) and BF (85.4231mg, 0.2774mmol). Similarly ternary co-crystals from the binary mixture DBDT, were prepared by adding halogen donors OF (76µL, 0.4159mmol), NF (71.59µL, 0.4159mmol), IF (167.1672mg, 0.4159mmol) and BF (128.0656mg, 0.4159mmol) i.e., in the ratio 1:2:2. These reactions were performed using a Labindia MM-1100 micro ball mill equipped with 1.5 ml stainless steel jars. The reactants were placed in a jar together with two stainless steel balls (5 mm diameter, 1 g each). 50 µL of methanol was added as the liquid (LAG) to the reaction mixture, which was then milled for 30 minutes at 25 Hz (1500 rpm) frequency. Recrystallization was done using suitable solvent systems.

3.2.3. CHARACTERISATION TECHNIQUES

Powder X-ray Diffraction: X-ray diffraction patterns were collected at room temperature on a Philips X'Pert Pro using Cu-Kα radiation (λ=1.54060 Å) in the 10-90° 2θ range (step size 0.0330°; time/step: 18.8700 s; 40 mA, 45 kV).

X-RAY DIFFRACTION:

X-ray diffraction is an analytical technique used for the determination of the atomic and molecular structure of a crystal, where a beam of X-rays incident on the crystal is diffracted into many specific directions. By measuring the angles and the intensities of the diffracted rays, it is possible to get information about the three-dimensional distribution of electron density within the crystal. From this, the mean positions of atoms as well as their chemical bond, their nature, their disorders can be determined.

X-ray diffraction is based on constructive interference of monochromatic X-rays and a crystalline sample. These X-rays are generated by a cathode ray tube, filtered to produce monochromatic radiation, collimated to concentrate, and directed toward the sample. The interaction of the incident rays with the sample produces constructive interference (and a diffracted ray) when conditions satisfy Bragg's Law ($n\lambda=2d\ \sin\theta$). This law relates the wavelength of electromagnetic radiation to the diffraction angle and the lattice spacing in a crystalline sample. These diffracted X-rays are then detected, processed and counted. By changing the geometry of the incident rays, the orientation of the centered crystal and the detector, all possible diffraction directions of the lattice should be attained. Crystalline solids consist of regular arrays of atoms, ions, or molecules with interatomic spacing on the order of 100 pm or 1 A. The wavelength of the incident light has to be in the same order as the spacing of the atoms. Reflection of X-rays only occurs when the conditions for constructive interference are fulfilled.

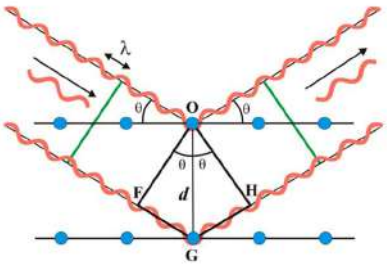

Fig.3.3: Diffraction of beams from different planes of the crystal.

Difference in path length = FG + GH

$$FG = GH = d_{hkl} \sin \theta_{hkl}$$

Difference in path length = $2d_{hkl} \sin \theta_{hkl}$, must be an integral number of wavelengths, $n\lambda = 2d_{hkl}\sin\theta_{hkl}$ (Where n is the order of diffraction and n=1,2,3…, λ is the wavelength of X ray beam, d is the interplanar distance, and θ is the incident angle) —Bragg's equation.

Modern X-ray diffractometers use a scintillation or CCD detector to record the angles and intensities of the diffracted beams. The resolution obtained by a diffractometer is better than photographic film, since the sample helps refocus the X-ray beam intensity is more readily measured and digitally stored.

Powder X-Ray Diffraction (PXRD):

A powder may be composed of many small and finely ground crystals, known as crystallites. These crystallites are assumed to be randomly oriented to one another. If the powder is placed in the path of a monochromatic X-ray beam, diffraction will occur from the planes in those crystallites that are oriented at the correct angle to fulfill the Bragg condition. The diffracted beams make an angle of 2θ with the incident beam.

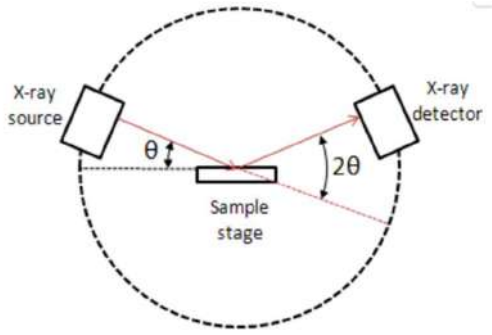

Fig.3.4: PXRD arrangement

The powder, sealed in a glass capillary tube, diffracts the X-rays (Bragg's law) to produce cones of diffracted beams. These cones intersect a strip of photographic film located in the cylindrical camera to produce a characteristic set of arcs on the film. The film can be removed and examined. Using the radius of the camera and the distance along with the film from the center, the Bragg angle 2θ and, therefore the d-spacing for each reflection can be calculated.

Hot-stage Microscopy: Thermal events of binary and ternary co-crystals of DB18C6 were observed on a hot-stage (THMS 600, Linkam Scientific Instruments Ltd, Surrey, UK) under an optical microscope mounted with a charge-coupled device (CCD) camera. Single crystals of the samples were placed on the sample stage and heated in the 30–300 °C temperature range at a rate of 20°C/min. The temperature of the hot-stage was monitored with a central processor (TMS 94, Linkam Scientific Instruments Ltd, Surrey, UK). Throughout heating, the morphological changes were recorded with CCD camera, and the data was imported into a computer for real-time observation and storage.

CHAPTER 4

RESULT AND DISCUSSION

4.1 Conformational analysis:

We used the Cambridge Structural Database (CSD) database for the conformational analysis of the crown ether series. With over twelve lakhs structural hits of organic and metal-organic structures, published across the publishers and years, it provides a rich resource for statistical analysis and data mining for crystal engineering and drug design activities. There are 214,39,11 and 11 hits for 18C6, DCH18C6, B18C6, and DB18C6, respectively. The VMD, is an open-access software used to visualize the conformations of various crown ethers in complexes. Accordingly, it is found that D_{3d}, C_i, C_1, and C_{2v} are the major conformations shown by the crown ether series themselves in respective complexes. With C_i, C_{2h}, C_1, C_2 as the less frequently observed conformations in the case of 18C6 and C_s, C_1, C_2 in the case of DCH18C6, and C_2 in the case of B18C6 and DB18C6. The frequency distribution of different conformations is presented below, along with a list of CCDC data (Appx. Table 4.1- 4.4).

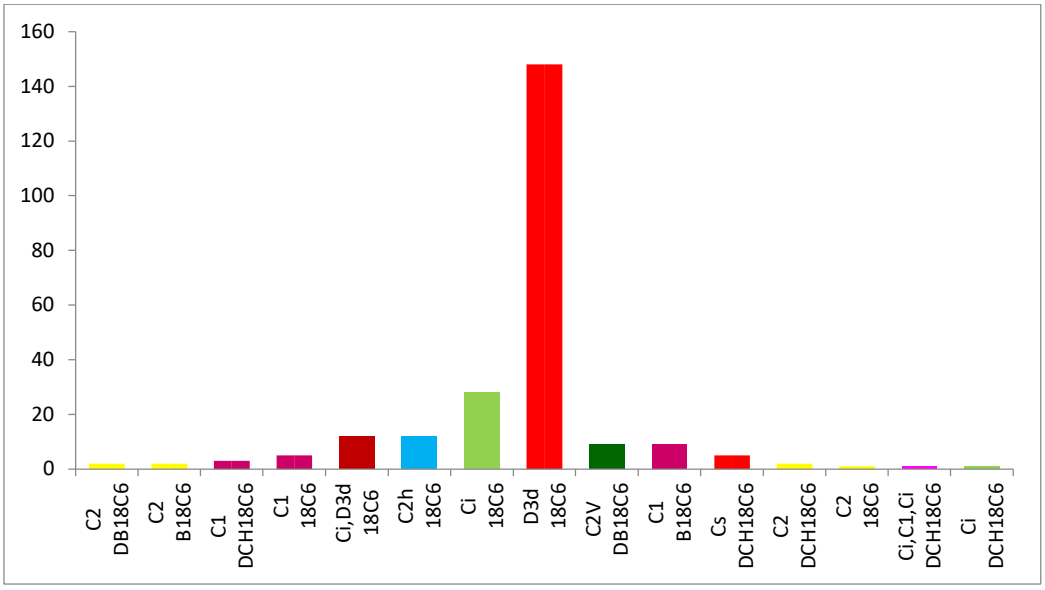

Fig. 4.1: Frequency distribution of various conformations from the table mentioned in appx.

The energy for various conformations is calculated using Gaussian 16W at the B3LYP/6-311++G(d,p) level. Calculations were done in the gaseous phase after normalizing hydrogen positions in the Mercury. Results are discussed below:

18C6

In 18C6, the most common conformations D_{3d} and C_i have comparable energies though that of D_{3d} is slightly higher (4.4 kcal/mol) compared to C_i (Fig.4.2) and could be due to the symmetry requirement of D_{3d} conformation with respect to C_i. The FIMs analysis also predicted the same trend. A comparison of the maps (Fig. 4.3) reveals that the D_{3d} conformation has a higher intensity than C_i, indicating that the D_{3d} is more accessible for hydrogen bonding.

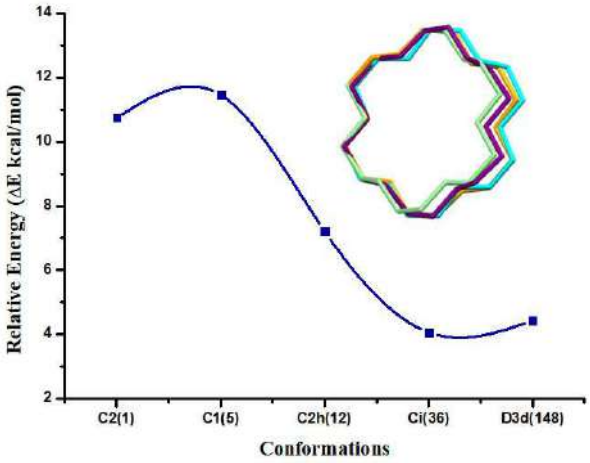

Fig.4.2: Graph showing relative energy of various conformations of 18C6. The numbers in brackets indicate the frequency distribution of various conformations. Structure overlay of several conformations is depicted in the figure. Colour code: Orange- D_{3d}, Light Green- C_i, Cyan- C_{2h}, Purple- C_1.

a) b)

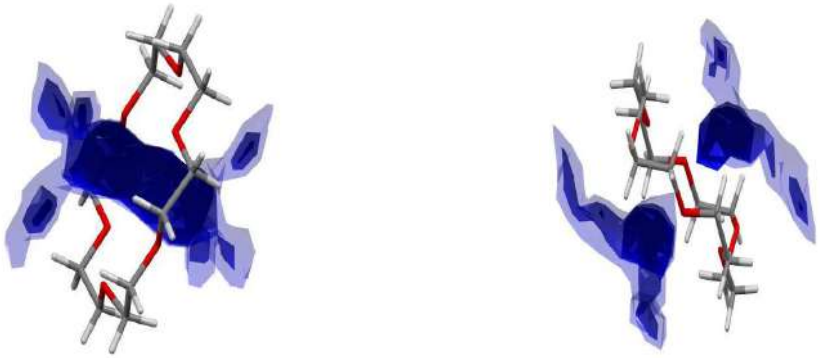

Fig.4.3: Full interaction map of a) D_{3d} b) C_i conformations of 18C6 with uncharged NH nitrogen.

C_{2h}, C_2, and C_1conformations are also observed in fewer numbers with a greater energy difference of 7.2, 10.7, and 11.5 kcal/mol, respectively. Thus, the distribution of all other conformations is clearly in accordance with its relative energy values.

DCH18C6

C_i, C_s, C_1, and C_2 are the mainly observed conformations of DCH18C6. The most frequent of these conformations are C_i and C_s. The relative energy values are consistent with this. C_i and C_s have relative energy of 6.4 and 8.9 kcal/mol, respectively, whereas C_2 and C_1 have slightly higher energy differences with the optimized energy, about 11.3 and 13.4 kcal/mol, respectively, which is in contradiction to their frequency distribution (Fig.4.4). The difference in interaction preferences brought about by the complexation (Uncharged NH) gives a clear picture of this anomaly (Fig.4.5). The interactions being more potent in C_1 conformation, as against C_2, make it a preferred conformation in the molecular complexes. Also, the symmetry constraints in the C_2make it challenging to incorporate into a crystal lattice compared to C_1, with no symmetry constraints.

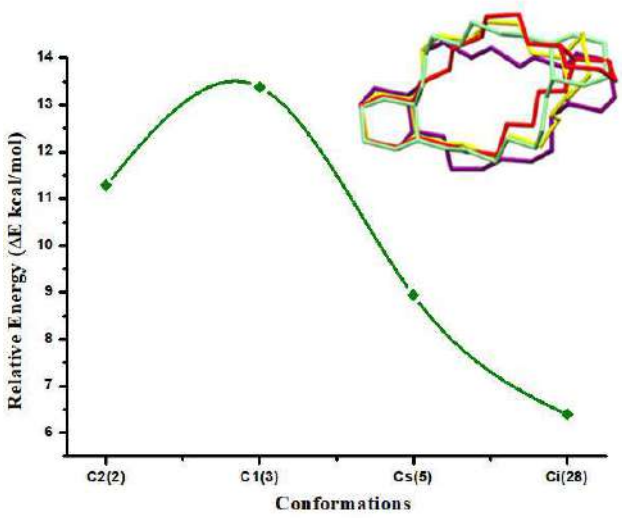

Fig.4.4: Graph showing relative energy of various conformations of DCH18C6. The numbers in brackets indicate the frequency distributions of various conformations. Structure overlay of several conformations is depicted in the figure. Colour code: Light Green- C_i, Violet- C_s, Purple- C_1, Yellow- C_2.

a) b)

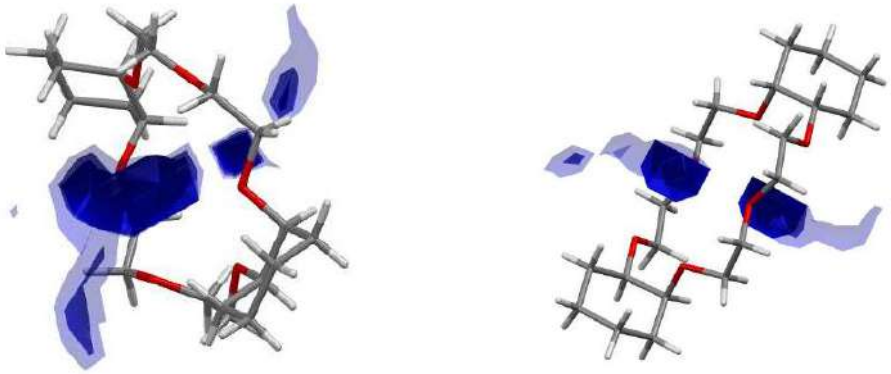

Fig.4.5: The calculated full interaction map of a) $C_1$and b) C_2 conformations of DCH18C6 with uncharged NH nitrogen.

B18C6:

The energy corresponding to the conformations supports its frequency distribution, suggesting that the complex formation occurs in accordance with the relative energy. C_1 conformation, the most frequently occurred, has the lowest relative energy (7.9 kcal/mol) and C_2 conformation less frequently occurred, has the highest relative energy (8.6 kcal/mol) (Fig.4.6). According to the full interaction map studies, although uncharged NH nitrogen has a lower intensity towards hydrogen bonding, alcoholic OH shows a higher intensity, indicating that the C_1 conformation is more accessible than the C_2 conformation.

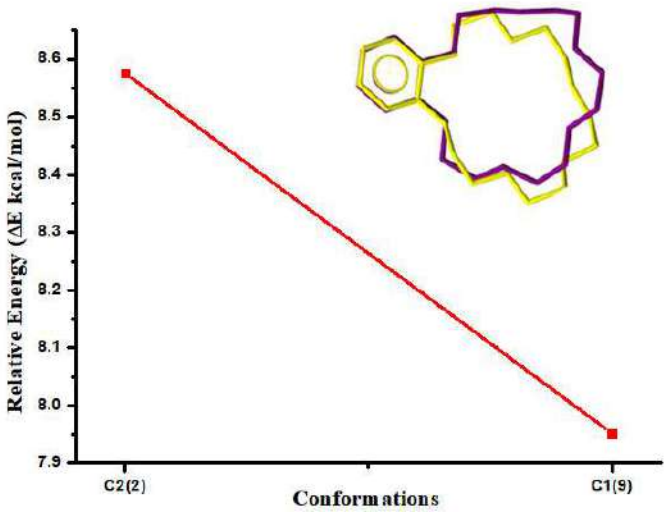

Fig.4.6: Graph showing relative energy of various conformations of B18C6. The numbers in brackets indicate the distribution of various conformations. Structure overlay of several conformations is depicted in the figure. Colour code: Purple- C_1, Yellow- C_2

a)

b)

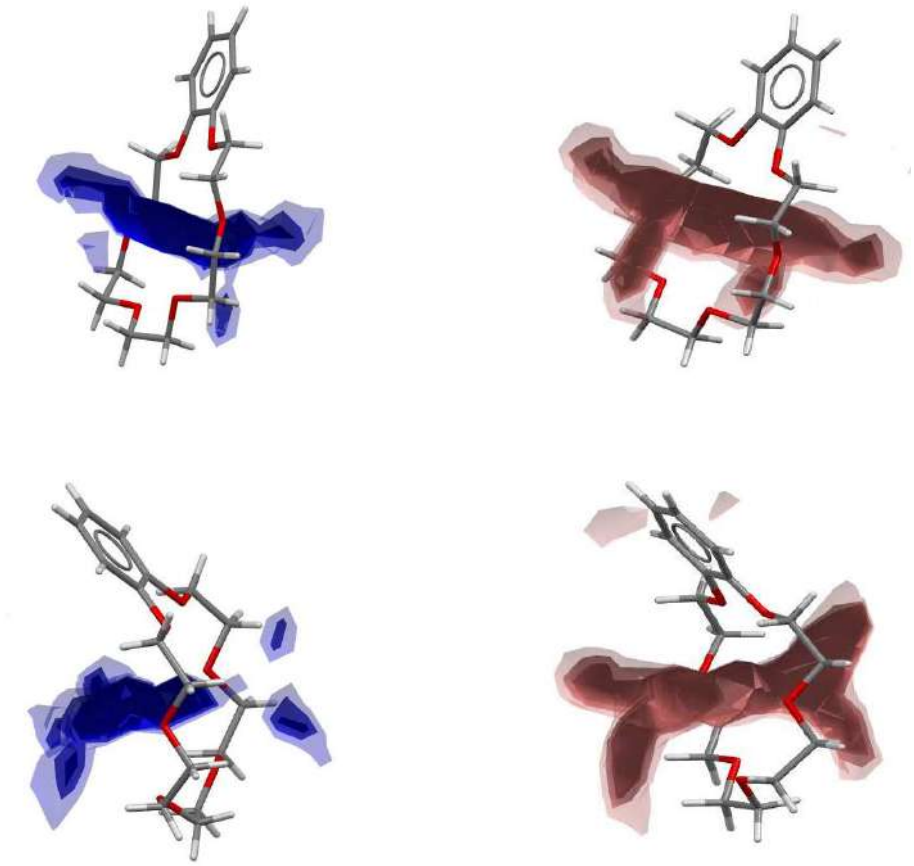

Fig.4.7: The calculated full interaction map of a) C_2 and b) C_1 conformations of B18C6 with uncharged NH(Blue) and Alcoholic OH (Brown).

DB18C6:

C_{2v} and C_2 conformations are the frequently observed conformations of DB18C6, and have relative energy of 4.8 and 6.3 kcal/mol, respectively (Fig.4.8). Energy values support the frequency distribution of each conformation. Full interaction map studies show the difference in interaction preferences on complexation (uncharged NH) in C_{2v} and C_2 conformations (Fig.4.9).

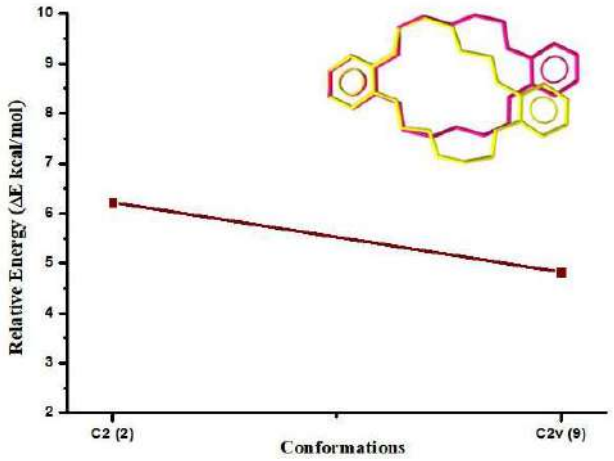

Fig.4.8: Graph showing relative energy of various conformations of DB18C6. The numbers in brackets indicate the distribution of various conformations. Structure overlay of several conformations is depicted in the figure. Colour code: Pink- C_{2v}, Yellow- C_2.

a) b)

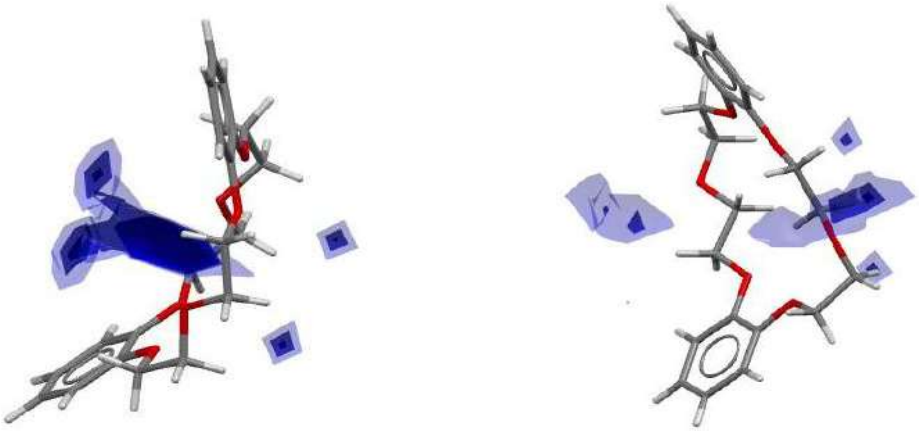

Fig.4.9: The calculated full interaction map of a) C_{2v} and b) C_2 conformations of DB18C6 with uncharged NH nitrogen.

4.2 Mechanochemical synthesis:

Binary co-crystals of DB18C6 with thiourea (TU) and dithiooxamide (DT)were prepared in the stoichiometric ratio 1:2 using mortar and pestle with methanol (50μ*L*) as a medium in liquid-assisted grinding (LAG) for 30 minutes. The presence of lone pairs of electrons on the sulfur atom, acting as acceptors, and the NH_2-hydrogen atoms as donors in TU and DT promote the formation of binary co-crystal. Ternary co-crystals were prepared with halogen donors such

as octafluoro-1,4-diiodobutane (OFIB), nonafluoro-1-iodobutane (NFIB), 1,4-Diiodotetrafluorobenzene (DITFB) and 1,4-Dibromotetrafluorobenzene (DBTFB) in the stoichiometric ratio 1:2:2 using micro ball mill, with methanol as added liquid, for 30 minutes. These halogen compounds are the strongest halogen bond donor groups. The polarizability of halogen atoms increases with an increase in size, F< Cl <Br <I. A fluorine atom with the least polarizability is less likely to act as a halogen bond donor, whereas an iodine atom strongly polarised acts as a strong halogen bond donor group. The presence of a neighboring fluorine atom increases the electron-accepting properties of the iodine and bromine atoms, thereby making strong halogen bonds. Thus, these four perfluorinated halogen bond donors include aliphatic and aromatic, monotopic and ditopic, linear and nonlinear, and iodine and bromine-based ones. The formation of co-crystals was confirmed by melting points and PXRD analysis.

The introduction of the two benzene groups on 18C6 restricts the conformational flexibility of the same. So, to the best of our knowledge, binary systems with DT or ternary systems with the aforementioned halogen compounds of DB18C6 have not been reported. Therefore, we conducted our work in an effort to refute this idea.

4.3 Hot-stage and optical microscope analysis:

The melting points of binary and ternary co-crystals were calculated using a hot-stage and an optical microscope. The melting points of the complexes lie either between or above that of the pure components, suggest the formation of co-crystals. For example, here, the melting point of DBTU is 170.2°C which is between the pure components, DB18C6(163.7°C) and TU (180.4°C). The melting point of DBDT is 179°C which is greater than the pure components, i.e., the melting point of DB18C6(163.7°C) and DT (166°C), indicating the formation of binary co-crystal. The melting point values of the ternary system are listed in the table below.

From the melting point values, it is found that the melting point of DBTUOF, DBTUIF and DBTUBF lies between the melting point of corresponding pure components and binary system indicating the formation of ternary systems. In the instance of DBDTIF and DBDTBF, we obtained the predicted melting point for DBDTBF but DBDTIF separated during recrystallisation in various solvent systems, despite the fact that we obtained the PXRD matching ternary system.

Table 4.5: Melting points of ternary co-crystals.

Melting point ($°C$)		
	DBTU (170.2°C)	DBDT (179°C)
OFDIB	150-153	_____
NFIB	_____	_____
DITFB (108°C -110°C)	160-163	110, 175
DBTFB (78°C -81°C)	158	240

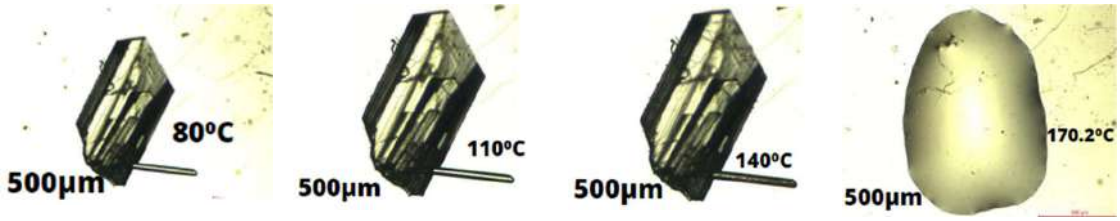

Fig 4.10: Phase transition accompanying melting of DBTU.

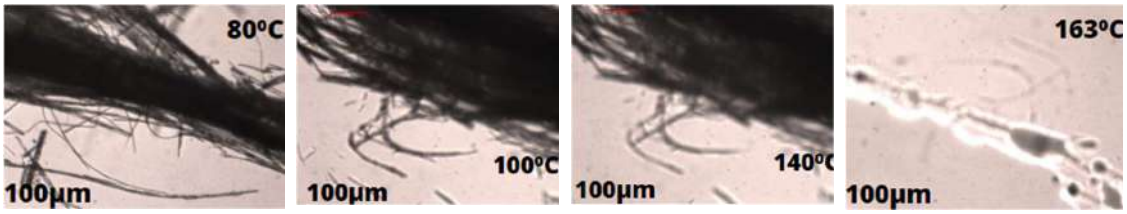

Fig 4.11: Phase transition accompanying melting of DBTUIF.

4.4 Powder XRD Data:

To validate the above presumption, we carried out a PXRD analysis. From PXRD patterns, we confirmed the crystalline nature and the formation of binary & ternary systems. In Fig.4.12, the characteristic peak at 2θ=11.9° indicates the successful formation of binary co-crystal DBTU. Characteristic peaks are observed in the case of DBTUOF, DBTUIF, and DBTUBF (Fig.4.12(a), (c), and (d)), suggesting the formation of ternary systems. There is no such characteristic peak creation in the case of DBTUNF (Fig.4.12(b)), and the patterns are comparable to those of the binary co-crystal, claiming no formation of ternary co-crystal. This

is because NFIB only has one iodine atom. Thus, we conclude that the ditopic halogen bond donors primarily generated the ternary co-crystals with DBTU.

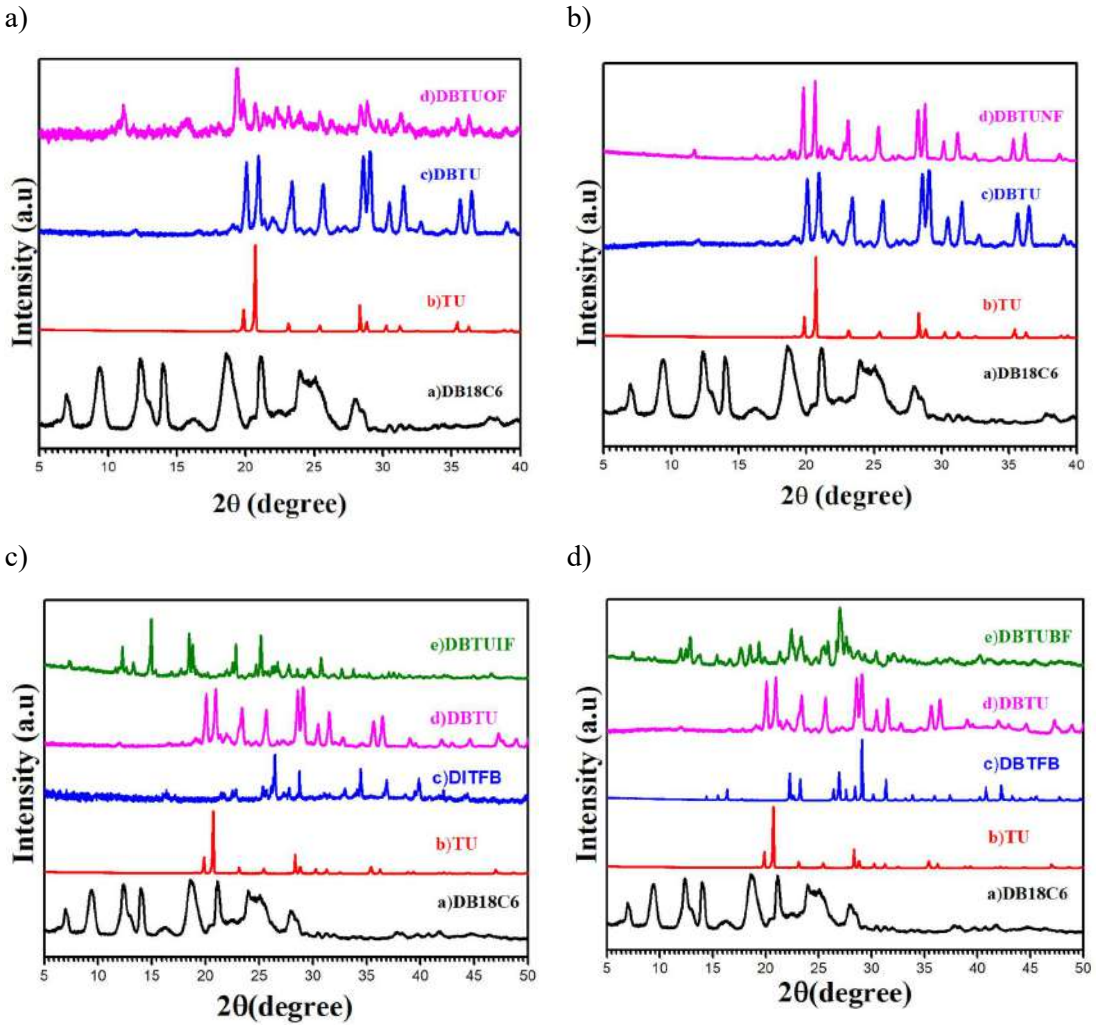

Fig.4.12: PXRD patterns of binary and ternary co-crystals of DB18C6 with TU.

Analyzing the PXRD patterns (Fig.4.13), the characteristic peak at 2θ=10.2° confirms the formation of binary co-crystal DBDT. The presence of two sulfur atoms (four lone pairs) and two NH_2 groups in dithiooxamide enhances the formation of robust hydrogen bonds, culminating in the formation of binary co-crystal. Unfortunately, PXRD patterns of DBDTOF and DBDTNF are comparable to that of the binary system DBDT(Fig.4.13(a) and (b)), suggesting no formation of the ternary system. However, in the case of DBDTIF and DBDTBF, distinctive peaks at 2θ=10.38° and 10.32°, respectively, indicate the successful formation of ternary co-crystals (Fig.4.13 (c) and (d)). In the instance of DBDT, the ternary system is thus created only with aromatic ditopic halogen bond donors.

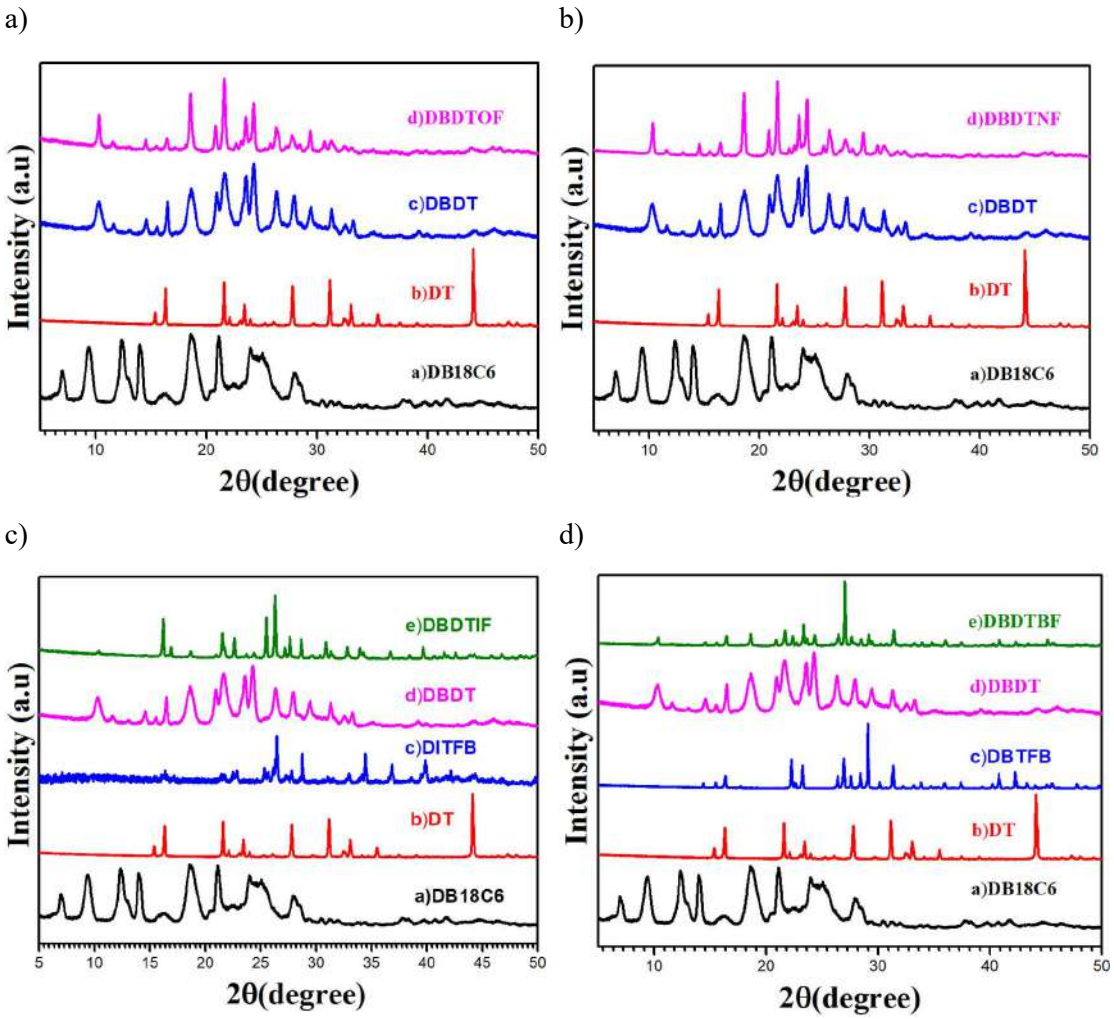

Fig.4.13: PXRD patterns of binary and ternary co-crystals of DB18C6 with DT.

CHAPTER 5

SUMMARY AND CONCLUSION

Conformational analysis of 18C6 series such as 18C6, DCH18C6, B18C6, and DB18C6 with neutral molecules was studied computationally. Studies show that most of the complexes fall under D_{3d}, C_i, $C_{1,}$ and C_{2v} conformations in the series, respectively. The computed energies and FIMs are in good agreement with the frequency distribution of the conformations. The investigation further validates the impact of conformations on cocrystallization.

To the best of our knowledge, DB18C6 has limited studies in the co-crystal formation and their structural evaluation due to the presence of two benzene rings, which reduces its flexibility. In the present work, we prepared binary and ternary co-crystals of DB18C6 using mechanochemical methods and characterized them using thermal and diffraction techniques. Distinct melting temperature infers the formation of binary and ternary co-crystals; usually, the T_m lies between or higher than the individual components. PXRD pattern analysis confirms the formation of ternary complexes in the case of DBTU, DBDT, DBTUOF, DBTUIF, DBTUBF, DBDTIF, and DBDTBF; but the systems such as DBTUNF, DBDTOF, and DBDTNF are confined to binary composition. Alternate methods such as POLAG will be employed to explore the ternary complexes for such systems. Based on the current experiments, we infer that the aromatic, ditopic halogen bond donors have a high potential for the formation of ternary co-crystals.

REFERENCES

(1) Desiraju, G. R. Crystal Engineering: From Molecule to Crystal. *J. Am. Chem. Soc.* **2013**, *135* (27), 9952–9967. https://doi.org/10.1021/ja403264c.

(2) Desiraju, G. R. Crystal Engineering: A Holistic View. *Angew. Chemie - Int. Ed.* **2007**, *46* (44), 8342–8356. https://doi.org/10.1002/anie.200700534.

(3) Liu, Z.; Nalluri, S. K. M.; Fraser Stoddart, J. Surveying Macrocyclic Chemistry: From Flexible Crown Ethers to Rigid Cyclophanes. *Chem. Soc. Rev.* **2017**, *46* (9), 2459–2478. https://doi.org/10.1039/c7cs00185a.

(4) Buckingham, A. D. Sir John Anthony Pople. 31 October 1925 — 15 March 2004. *Biogr. Mem. Fellows R. Soc.* **2006**, *52* (0), 299–314. https://doi.org/10.1098/rsbm.2006.0021.

(5) Schlexer Lamoureux, P.; Winther, K. T.; Garrido Torres, J. A.; Streibel, V.; Zhao, M.; Bajdich, M.; Abild-Pedersen, F.; Bligaard, T. Machine Learning for Computational Heterogeneous Catalysis. *ChemCatChem.* **2019**, *11* (16), 3581–3601. https://doi.org/10.1002/cctc.201900595.

(6) Barannikov, V. P.; Guseinov, S. S.; V'ugin, A. I. Molecular Complexes of Crown Ethers in Crystals and Solutions. *Russ. J. Coord. Chem. Khimiya.* **2002**, *28* (3), 153–162. https://doi.org/10.1023/A:1014729400394.

(7) Shan, N.; Toda, F.; Jones, W. Mechanochemistry and Co-Crystal Formation: Effect of Solvent on Reaction Kinetics. *Chem. Commun.* **2002**, *2* (20), 2372–2373. https://doi.org/10.1039/b207369m.

(8) Braga, D.; Maini, L.; Grepioni, F. Mechanochemical Preparation of Co-Crystals. *Chem. Soc. Rev.* **2013**, *42* (18), 7638–7648. https://doi.org/10.1039/c3cs60014a.

(9) Aitipamula, S.; Banerjee, R.; Bansal, A. K.; Biradha, K.; Cheney, M. L.; Choudhury, A. R.; Desiraju, G. R.; Dikundwar, A. G.; Dubey, R.; Duggirala, N.; Ghogale, P. P.; Ghosh, S.; Goswami, P. K.; Goud, N. R.; Jetti, R. R. K. R.; Karpinski, P.; Kaushik, P.; Kumar, D.; Kumar, V.; Moulton, B.; Mukherjee, A.; Mukherjee, G.; Myerson, A. S.; Puri, V.; Ramanan, A.; Rajamannar, T.; Reddy, C. M.; Rodriguez-Hornedo, N.; Rogers, R. D.; Row, T. N. G.; Sanphui, P.; Shan, N.; Shete, G.; Singh, A.; Sun, C. C.; Swift, J. A.;

Thaimattam, R.; Thakur, T. S.; Kumar Thaper, R.; Thomas, S. P.; Tothadi, S.; Vangala, V. R.; Variankaval, N.; Vishweshwar, P.; Weyna, D. R.; Zaworotko, M. J. Polymorphs, Salts, and Co-crystals: What's in a Name? *Cryst. Growth Des.* **2012**, *12* (5), 2147–2152. https://doi.org/10.1021/cg3002948.

(10) Friščič, T.; Jones, W. Recent Advances in Understanding the Mechanism of Cocrystal Formation via Grinding. *Cryst. Growth Des.* **2009**, *9* (3), 1621–1637. https://doi.org/10.1021/cg800764n.

(11) Trask, A. V.; Motherwell, W. D. S.; Jones, W. Solvent-Drop Grinding: Green Polymorph Control of Cocrystallisation. *Chem. Commun.* **2004**, *4* (7), 890–891. https://doi.org/10.1039/b400978a.

(12) Fischer, F.; Fendel, N.; Greiser, S.; Rademann, K.; Emmerling, F. Impact Is Important-Systematic Investigation of the Influence of Milling Balls in Mechanochemical Reactions. *Org. Process Res. Dev.* **2017**, *21* (4), 655–659. https://doi.org/10.1021/acs.oprd.6b00435.

(13) Julien, P. A.; Malvestiti, I.; Friš, T. The Effect of Milling Frequency on a Mechanochemical Organic Reaction Monitored by in Situ Raman Spectroscopy. *Beilstein J. Org. Chem.* **2017**, *13*, 2160–2168. https://doi.org/10.3762/bjoc.13.216.

(14) Friić, T.; Childs, S. L.; Rizvi, S. A. A.; Jones, W. The Role of Solvent in Mechanochemical and Sonochemical Cocrystal Formation: A Solubility-Based Approach for Predicting Cocrystallisation Outcome. *CrystEngComm*.**2009**, *11* (3), 418–426. https://doi.org/10.1039/b815174a.

(15) Friščić, T.; Mottillo, C.; Titi, H. M. Mechanochemistry for Synthesis. *Angew. Chemie.* **2020**, *132* (3), 1030–1041. https://doi.org/10.1002/ange.201906755.

(16) Do, J. L.; Friščić, T. Mechanochemistry: A Force of Synthesis. *ACS Cent. Sci.* **2017**, *3* (1), 13–19. https://doi.org/10.1021/acscentsci.6b00277.

(17) Foster, R.; Fyfe, C. A. Chapter 1 Nuclear Magnetic Resonance of Organic Charge-Transfer Complexes. *Prog. Nucl. Magn. Reson. Spectrosc.* **1969**, *4* (C), 1–89. https://doi.org/10.1016/0079-6565(69)80002-6.

(18) Metrangolo, P.; Neukirch, H.; Pilati, T.; Resnati, G. Halogen Bonding Based Recognition

Processes: A World Parallel to Hydrogen Bonding. *Acc. Chem. Res.* **2005**, *38* (5), 386–395. https://doi.org/10.1021/ar0400995.

(19) Mukherjee, A., Tothadi, S., & Desiraju, G. R. Halogen Bonds in Crystal Engineering: Like Hydrogen Bonds yet Different. *Acc. Chem. Res.* **2014,** *47*(8), 2514–2524 doi:10.1021/ar5001555.

(20) Dale, J. The Conformation of Free and Complexed Oligoethers. *Isr. J. Chem.* **1980**, *20* (1–2), 3–11. https://doi.org/10.1002/ijch.198000047.

(21) Al-Jallal, N. A.; Al-Kahtani, A. A.; El-Azhary, A. A. Conformational Study of the Structure of Free 18-Crown-6. *J. Phys. Chem. A* **2005**, *109* (16), 3694–3703. https://doi.org/10.1021/jp050133c.

(22) Leuwerink, F. T. H.; Briels, W. J. The Dipole Moment of 18-Crown-6: Molecular Dynamics Study of the Structure and Dynamics of the Macrocycle in Vacuo and in Cyclohexane. *J. Chem. Phys.* **1995**, *103* (11), 4637–4652. https://doi.org/10.1063/1.470652.

(23) Wipff, G., Weiner, P., & Kollman, P. A molecular-mechanics study of 18-crown-6 and its alkali complexes: an analysis of structural flexibility, ligand specificity, and the macrocyclic effect. *J. Am. Chem. Soc.* **1983**, *104,* (12), 3249–3258. doi:10.1021/ja00376a001.

(24) Bombieri, G.; de Paoli, G.; Benetollo, F.; Cassol, A. Crown Ether Complexes of Lanthanoid and Actinoid Elements. Crystal and Molecular Structure of Nd(NO3)3 (18-Crown-6). *J. Inorg. Nucl. Chem.* **1980**, *42* (10), 1417–1422. https://doi.org/10.1016/0022-1902(80)80107-2.

(25) Takeuchi, H., Arai, T., & Harada, I. Structures of 18-crown-6, 15-crown-5 and their metal complexes in methanol solution as studied by Raman spectroscopy. *J. Mol. Struct.* **1986**, 146, 197–212. doi:10.1016/0022-2860(86)80293-9.

(26) Dalley, N. K., Smith, D. E., Izatt, R. M., & Christensen, J. J. X-Ray crystal structure of the barium thiocyanate complex of the cyclic poly-ether dicyclohexyl-18-crown-6 (isomer A). *Chem. Commun.***1972**, (2), 90-91. doi:10.1039/c39720000090.

(27) Navaza, A.; Villain, F.; Charpin, P. Crystal Structures of the Dicyclohexyl-(18-Crown-6) Uranyl Perchlorate Complex and of Its Hydrolysis Product. *Polyhedron* **1984**, *3* (2), 143–149. https://doi.org/10.1016/S0277-5387(00)88043-2.

(28) Kusaka, R.; Inokuchi, Y.; Ebata, T. Water-Mediated Conformer Optimization in Benzo-18-Crown-6-Ether/Water System. *Phys. Chem. Chem. Phys.* **2009**, *11* (40), 9132–9140. https://doi.org/10.1039/b909618c.

(29) Harkema, S.; Van Hummel, G. J.; Daasvatn, K.; Reinhoudt, D. N. Complexes of Crown Ethers and Neutral Molecules; Synthesis and Crystal Structure of a Urea 18-Crown-6 (5:1) Complex. *Chem. Commun.* **1981**, No. 8, 368–369. https://doi.org/10.1039/c39810000368.

(30) Drew, M. G. B., & Nicholson, D. G. Structure of a 1:2 adduct between 1,4,7,10,13,16-hexaoxacyclooctadecane (18-crown-6) and thiourea, C12H24O6.2CH4N2S.*Acta Crystallogr. C Struct. Chem.* **1985**, *41*(9), 1358–1360. doi:10.1107/s0108270185007764.

(31) Topić, F.; Rissanen, K. Systematic Construction of Ternary Co-crystals by Orthogonal and Robust Hydrogen and Halogen Bonds. *J. Am. Chem. Soc.* **2016**, *138* (20), 6610–6616. https://doi.org/10.1021/jacs.6b02854.

(32) Chulanova, E. A.; Radiush, E. A.; Shundrina, I. K.; Bagryanskaya, I. Y.; Semenov, N. A.; Beckmann, J.; Gritsan, N. P.; Zibarev, A. V. Lewis Ambiphilicity of 1,2,5-Chalcogenadiazoles for Crystal Engineering: Complexes with Crown Ethers. *Cryst. Growth Des.* **2020**, *20* (9), 5868–5879. https://doi.org/10.1021/acs.cgd.0c00536.

(33) Faure, A.; Gorfinkiel, J. D.; Morgan, L. A.; Tennyson, J. GTOBAS: Fitting Continuum Functions with Gaussian-Type Orbitals. *Comput. Phys. Commun.* **2002**, *144* (2), 224–241. https://doi.org/10.1016/S0010-4655(02)00141-8.

(34) Jensen, F. Introduction to Computational Chemistry, 3rd Edn. Wiley & Sons, **2013**.

APPENDIX

Table 4.1: Summary of various conformations of 18C6 with neutral molecules obtained from CSD database.

No:	***Refcode***	***Space Gp.***	**18-CROWN-6; No error; No ions; No disorders; only organic; Hits -214** ***Compound Name (L)***	***Confor-mations***
1.	OGIMID	*P*-1	[1,2,5]thiadiazolo[3,4-c][1,2,5]thiadiazolo 18-crown-6	D_{3d}
2.	APARUH	$P2_12_12_1$	ammine(formato)dihydridoboron 18-crown-6	D_{3d}
3.	BAPRAM	$P2_1/c$	1,4,7,10,13,16-Hexaoxacyclooctadecane bis(1-(2-aminobenzoyl)thiosemicarbazide) clathrate	D_{3d}
4.	BECXUE	*Pbca*	bis(benzoyl(hydroxyimino)acetonitrile) 18-crown-6 tetrahydrate	D_{3d}
5.	BEJPAH	$P2_1/c$	1,4,7,10,13,16-Hexaoxacyclo-octadecane phenylcarbamate clathrate	D_{3d}
6.	BIJWAS	$P2_1/n$	18-Crown-6 bis(nitromethane) clathrate	D_{3d}
7.	BIJWAS01	$P2_1/n$	18-Crown-6 bis(nitromethane) clathrate	D_{3d}
8.	BIJWAS02	$P2_1/n$	18-Crown-6 bis(nitromethane) clathrate	D_{3d}
9.	BIJWAS03	$P2_1/n$	1,4,7,10,13,16-Hexaoxacyclooctadecane bis(nitromethane) clathrate	D_{3d}
10.	BIJWAS04	$P2_1/n$	1,4,7,10,13,16-Hexaoxacyclooctadecane bis(nitromethane) clathrate	D_{3d}
11.	BIJWAS05	$P2_1/n$	1,4,7,10,13,16-Hexaoxacyclooctadecane bis(nitromethane) clathrate	D_{3d}
12.	BIJWAS06	$P2_1/n$	1,4,7,10,13,16-Hexaoxacyclooctadecane bis(nitromethane) clathrate	D_{3d}
13.	BIJWAS07	$P2_1/n$	1,4,7,10,13,16-Hexaoxacyclooctadecane bis(nitromethane) clathrate	D_{3d}
14.	BIJWAS08	$P2_1/n$	1,4,7,10,13,16-Hexaoxacyclooctadecane bis(nitromethane) clathrate	D_{3d}
15.	BIJWAS09	$P2_1/n$	1,4,7,10,13,16-Hexaoxacyclooctadecane bis(nitromethane) clathrate	D_{3d}
16.	BIJWAS10	$P2_1/n$	1,4,7,10,13,16-Hexaoxacyclooctadecane bis(nitromethane) clathrate	D_{3d}

17.	BIZPIL	$P2_1$	18-Crown-6 difluoro(2-oxybenzamidinium)pborate	D_{3d}
18.	BOBVUL	*P*-1	bis(Phosphinecarboxamide) 1,4,7,10,13,16-hexaoxacyclooctadecane	D_{3d}
19.	BUPRAF	$P2_1/c$	1,4,7,10,13,16-Hexaoxacyclo-octadecane bis(N,N'-dimethylthiourea) clathrate	D_{3d}
20.	CEDZAM	$P2_12_12_1$	Amminetrifluoroboron 1,4,7,10,13,16-hexaoxacyclo-octadecane dichloromethane solvate	D_{3d}
21.	CEHGEB	*P*-1	18-Crown-6 bis(formamide)	D_{3d}
22.	CEHGEB01	*P*-1	18-crown-6 bis(formamide)	D_{3d}
23.	CEHGUR	$P2_1/c$	18-Crown-6 bis(3-nitrophenol) dihydrate	D_{3d}
24.	CEHHAY	$P2_1/c$	18-Crown-6 bis(p-nitrobenzaldehyde oxime) dihydrate	D_{3d}
25.	CEJVIW	$P2_1/n$	1,4,7,10,13,16-Hexaoxacyclo-octadecane N,N'-diformohydrazide	D_{3d}
26.	CEKXUL	*P*-1	1,4,7,10,13,16-Hexaoxacyclo-octadecane bis(2,4-dinitrophenol) clathrate dihydrate	D_{3d}
27.	CENGUX	$P2_1/n$	18-Crown-6 cyano-acetic acid clathrate monohydrate	D_{3d}
28.	CENHAE	$P2_1/c$	18-Crown-6 bis(cyanamide) clathrate	D_{3d}
29.	CENHAE01	$P2_1/c$	18-Crown-6 bis(cyanamide) clathrate	D_{3d}
30.	CENHAE02	$P2_1/c$	18-Crown-6 bis(cyanamide) clathrate	D_{3d}
31.	CENHEI	$P2_1/n$	18-Crown-6 bis(1-chloroethylsulfonamide) clathrate	D_{3d}
32.	CICVUF	$C2/c$	1,4,7,10,13,16-Hexaoxacyclo-octadecane bis(2-(2-benzimidazolyl)-guanidine) clathrate	D_{3d}
33.	CIRTEC01	$P2_1/a$	1,4,7,10,13,16-Hexaoxacyclo-octadecane bis(dichloropicric acid) dihydrate	D_{3d}
34.	CIRTEC02	$C2/c$	1,4,7,10,13,16-Hexaoxacyclo-octadecane bis(dichloropicric acid) dihydrate	D_{3d}
35.	CRHYDZ	$P2_1/c$	1,4,7,10,13,16-Hexaoxacyclo-octadecane bis(2,4-dinitrophenylhydrazine) clathrate	D_{3d}
36.	CRMESF	$P2_1/n$	1,4,7,10,13,16-Hexaoxacyclo-octadecane bis(dimethylsulfone) clathrate	D_{3d}

37.	CRPACX10	*P*-1	1,4,7,10,13,16-Hexaoxacyclo-octadecane dimethylacetylenedicarboxylate	D_{3d}
38.	DAFGOJ	*C*2/*c*	2,6-diamino-4-chloro-3,5-difluoropyridine hemikis(18-crown-6)	D_{3d}
39.	DAYWIJ	*P*-1	1,4,7,10,13,16-Hexaoxacyclo-octadecane bis(thiourea) clathrate	D_{3d}
40.	DEJXAR	$Pna2_1$	18-Crown-6 amidosulfuric acid ethanol solvate	D_{3d}
41.	DUKREJ	$P2_1/n$	18-crown-6 1,2,4,5-tetrafluoro-3,6-di-iodobenzene acetonitrile solvate	D_{3d}
42.	ECICEY	$P2_1/n$	(18-Crown-6) 4-amino-3-ethoxycarbonyl-1,2,5-oxadiazole	D_{3d}
43.	ECICIC	*P*-1	(18-Crown-6) bis(4-(2-chloroethylamino)-3-carbhydrazido-1,2,5-oxadiazole)	D_{3d}
44.	EMISID	*P*-1	18-crown-6 bis((mu!2$-amino)-(mu!2$-hydrido)-diborane)	D_{3d}
45.	EMISOJ	$P2_12_12_1$	18-crown-6 (amine)-((borane)amino)borane	D_{3d}
46.	EMISOJ01	$P2_12_12_1$	18-crown-6 amino(boranylamino)borane	D_{3d}
47.	EMISOJ02	$P2_12_12_1$	18-crown-6 amino(boranylamino)borane	D_{3d}
48.	EPAQES	*C*2/*m*	2,3,5,6-Tetrafluorobenzene-1,4-diamine 1,4,7,10,13,16-hexaoxacyclooctadecane	D_{3d}
49.	EREMEW	$P2_1/n$	(18-crown-6) bis(ammine-(chloroacetato)-dihydrido-boron)	D_{3d}
50.	GEFREO	*P*-1	18-Crown-6 bis(acetonitrile) clathrate	D_{3d}
51.	GEFREO02	$P2_1/n$	18-Crown-6 bis(acetonitrile) clathrate	D_{3d}
52.	GEFREO09	*P*-1	18-crown-6 acetonitrile solvate	D_{3d}
53.	GOJZUC	$P2_1/n$	Cyanic thiocyanate 1,4,7,10,13,16-hexaoxacyclo-octadecane	D_{3d}
54.	HADMOO	*I*2/*c*	bis(4-Amino-N-(5-methoxy-2-pyrimidinyl)benzenesulfonamide)-1,4,7,10,13,16-hexaoxacyclo-octadecane tetra-acetonitrile clathrate	D_{3d}
55.	HADMUU	$P2_1/n$	4-Amino-N-(2-thiazolyl)benzenesulfonamide (18-crown-6) acetonitrile clathrate	D_{3d}
56.	HADNAB	$P2_1/c$	bis(4-Amino-N-(4-methyl-2-pyrimidinyl)benzenesulfonamide) (18-crown-6) diacetonitrile clathrate	D_{3d}

57.	HODMLN	$P2_1/c$	1,4,7,10,13,16-Hexaoxacyclo-octadecane bis(malononitrile)	D_{3d}
58.	HOXBSA01	$P2_1/n$	bis(benzenesulfonamide) 1,4,7,10,13,16-hexaoxacyclooctadecane	D_{3d}
59.	IKAWUM	$P2_1/c$	1,4,7,10,13,16-Hexaoxacyclo-octadecanebis(2-(quinoline-2-lcarbonyl)hydrazinecarbothioamide) clathrate	D_{3d}
60.	IRUKIS	$P2_1/c$	phosphanecarbohydrazide hemikis(18-crown-6)	D_{3d}
61.	ITOPEN	P-1	tris(Pentafluorophenyl)(tetrahydrofuran)borate hemikis(18-crown-6)	D_{3d}
62.	IVIGAW	$C2/c$	1,3,4,5,6,8-Hexafluoronaphthalene-2,7-diamine 1,4,7,10,13,16-hexaoxacyclooctadecane	D_{3d}
63.	JAPFOW	$P2_1/c$	1,4,7,10,13,16-Hexaoxacyclo-octadecanebis(6-chloro-4-nitroso-3,4-dihydro-2H-1,2,4-benzothiadiazine-7-sulfonamide 1,1-dioxide) clathrate	D_{3d}
64.	JEDPOY	R-3m	Poly(cis,cis-cyclohexane-1,3,5-tricarboxylic acid) hemikis(18-crown-6) clathrate	D_{3d}
65.	JIBNUD	P-1	bis(5-Acetamido-1,3,4-thiadiazole-2-sulfonamide) 18-crown-6 clathrate	D_{3d}
66.	KATLAT	$P2_1/c$	bis(Ammonia) 1,4,7,10,13,16-hexaoxacyclooctadecane	D_{3d}
67.	KATLAT01	$P2_1/c$	1,4,7,10,13,16-Hexaoxacyclo-octadecane bis(ammonia)	D_{3d}
68.	KEZYUJ	P-1	18-Crown-6 chlorobis(methylsulfonyl)amine clathrate	D_{3d}
69.	KEZZAQ	$P2_1/c$	18-Crown-6 methylbis(methylsulfonyl)amine clathrate	D_{3d}
70.	KEZZIY	P-1	18-Crown-6 bis(methylbis(methylsulfonyl)amine) clathrate	D_{3d}
71.	KEZZOE	P-1	18-Crown-6 (methylsulfonyl)(phenylsulfonyl)amine dimethylsulfoxide clathrate	D_{3d}
72.	KIBBEC	P-1	18-Crown-6 bis(bis(methylsulfonyl)amine) dimethylsulfoxide monohydrate clathrate	D_{3d}
73.	KOPYET	$P2_1/n$	1,4,7,10,13,16-Hexaoxacyclo-octadecane bis(fluoroacetonitrile) clathrate	D_{3d}
74.	KOTGAE	$Pca2_1$	5-nitrobenzene-1,3-dicarboxylic acid 18-crown-6 trihydrate	D_{3d}
75.	LEKYIJ	P-1	18-Crown-6 bis(aqua-trifluoroboron(iii)) dihydrate	D_{3d}
76.	MOBYEJ	$P2_1/n$	1,4,7,10,13,16-Hexaoxacyclooctadecane bis(iodomethane) clathrate	D_{3d}

77.	MOBYEJ01	$P2_1/n$	1,4,7,10,13,16-Hexaoxacyclooctadecane bis(iodomethane) clathrate	D_{3d}
78.	MOBYEJ03	$P2_1/n$	18-crown-6 bis(iodomethane)	D_{3d}
79.	MOBYEJ04	$P2_1/n$	18-crown-6 bis(iodomethane)	D_{3d}
80.	MOBYEJ05	$P2_1/n$	18-crown-6 bis(iodomethane)	D_{3d}
81.	MOBYEJ06	$P2_1/n$	18-crown-6 bis(iodomethane)	D_{3d}
82.	MOBYEJ07	$P2_1/n$	18-crown-6 bis(iodomethane)	D_{3d}
83.	MOBYEJ08	$P2_1/n$	18-crown-6 bis(iodomethane)	D_{3d}
84.	MUJFIG	$P2_1/n$	bis(2-Aminobenzoic acid hydrazide) 18-crown-6 dihydrate	D_{3d}
85.	MUJFOM	*Pbca*	bis(5-Amino-1-benzyl-1,2,3-triazole-4-carbonic acid hydrazide) 18-crown-6	D_{3d}
86.	NEWPIP	*Cc*	1,4,7,10,13,16-Hexaoxacyclo-octadecane 3-thioamidopyridine clathrate	D_{3d}
87.	NURHIR	$P2_1/c$	1,4,7,10,13,16-Hexaoxacyclo-octadecane bis(formic acid)	D_{3d}
88.	OGIMUP	$P2_1/c$	1,2,5-telluradiazole-3,4-dicarbonitrile 18-crown-6	D_{3d}
89.	OQITIT	*P*-1	(18-Crown-6) bis(thiourea) bis(1,2,3,4-tetrafluoro-5,6-diiodobenzene)	D_{3d}
90.	OQITOZ	$P2_1/c$	(18-Crown-6) bis(thiourea) bis(1,2,4,5-tetrafluoro-3,6-diiodobenzene)	D_{3d}
91.	OQITUF	$P2_1/c$	(18-Crown-6) bis(thiourea) bis(1,2,4,5-tetrafluoro-3,6-dibromobenzene)	D_{3d}
92.	OSAMEC	$P2_1/n$	18-crown-6 bis(iodomethane)	D_{3d}
93.	PAVPUX	$P2_12_12_1$	L-alpha-Alanyl-L-alpha-alanine 18-crown-6 dihydrate	D_{3d}
94.	PEGXAC	$P2_1/n$	,4,7,10,13,16-hexaoxacyclooctadecane 3,5,6-trifluoropyridine-2,4-diamine	D_{3d}
95.	PEGXEG	*Pbca*	1,4,7,10,13,16-hexaoxacyclooctadecane 3,6-difluoropyridine-2,4-diamine	D_{3d}
96.	PEGXOQ	*P*-1	1,4,7,10,13,16-hexaoxacyclooctadecane 3,5-difluoropyridine-2,6-diamine	D_{3d}
97.	PEGXUW	*C*2/*c*	1,4,7,10,13,16-hexaoxacyclooctadecane 4-chloro-3,5-difluoropyridine-2,6-diamine	D_{3d}

98.	POMCOJ	$P2_1/n$	1,4,7,10,13,16-Hexaoxacyclo-octadecane dimesylamine	D_{3d}
99.	PUNWED	P-1	pentafluorophenol 18-crown-6 tetrahydrate	D_{3d}
100.	PUNWIH	$P2_1/c$	pentafluorophenol 18-crown-6 dihydrate	D_{3d}
101.	PUNWON	$P2_1/c$	pentafluorobenzoic acid 18-crown-6 dihydrate	D_{3d}
102.	PUNXAA	P-1	1,4-dihydroxy-tetrafluorobenzene 18-crown-6 dihydrate	D_{3d}
103.	PUNXII	P-1	4-amino-2,3,5,6-tetrafluorobenzoic acid 18-crown-6 monohydrate	D_{3d}
104.	PUVVOR	P-1	1,4,7,10,13,16-Hexaoxacyclo-octadecane bis(dimethyl sulfoxide) bis(bis(4-fluorophenylsulfonyl)amine)	D_{3d}
105.	QADYAW	P-1	18-Crown-6 dinitric acid dihydrate clathrate	D_{3d}
106.	QADYAW01	P-1	18-Crown-6 dinitric acid dihydrate clathrate	D_{3d}
107.	REGRAW01	$P2_1/c$	1,4,7,10,13,16-Hexaoxacyclooctadecane tetrahydrate	D_{3d}
108.	RILVIR	P-1	(18-Crown-6) bis(4-carboxybenzenesulfonyl)amine tetrahydrate	D_{3d}
109.	RIYVEB	$P2_1/c$	bis(2-(Mesitylmethylsulfanyl)pyridine N-oxide) 18-crown-6	D_{3d}
110.	SIXTEY	Cc	18-Crown-6 maleic acid dihydrate	D_{3d}
111.	SOVJOC	$P2_12_12_1$	18-Crown-6 aminosulfuric acid clathrate	D_{3d}
112.	SOVYAG	$P2_1/c$	bis(3,5,6-trifluoropyridin-2-amine) 18-crown-6	D_{3d}
113.	SOVYEK	C2/c	bis(4-chloro-3,5,6-trifluoropyridin-2-amine) 18-crown-6	D_{3d}
114.	SOVYIO	$P2_1/n$	bis(5,7-difluoroquinolin-2-amine) 18-crown-6	D_{3d}
115.	SOVYOU	$P2_1/n$	bis(2-chloro-5,6,8-trifluoroquinolin-7-amine) 18-crown-6	D_{3d}
116.	SOVYUA	$P2_1/c$	bis(N$4!-[(anthracen-9-yl)methyl]-3,5,6-trifluoropyridine-2,4-diamine) 18-crown-6	D_{3d}
117.	SOWKEX	$P2_1$	18-crown-6 bis(hydrazine)	D_{3d}
118.	TONFIL	$P2_1/n$	18-Crown-6 3,4-diaminofurazane clathrate monohydrate	D_{3d}

119.	TUJKOY	*P*-1	18-Crown-6 bis(N-methyl(benzenesulfonyl)(methanesulfonyl)amine)	D_{3d}
120.	VAVLUZ	$P2_1/n$	18-Crown-6 benzenesulfonamide clathrate	D_{3d}
121.	VAVLUZ01	$P2_1/n$	benzenesulfonamide 1,4,7,10,13,16-hexaoxacyclooctadecane	D_{3d}
122.	VEPWOF	*P*-1	bis(1,3,4,5,6,7,8-heptafluoronaphthalen-2-amine) 18-crown-6	D_{3d}
123.	VEPWUL	*P*-1	bis(pentafluoroaniline) 18-crown-6	D_{3d}
124.	VEPXAS	*P*-1	bis(2,3,5,6-tetrafluoroaniline) 18-crown-6	D_{3d}
125.	VEVYAW	$P2_1/a$	18-Crown-6 hydroquinone clathrate hexahydrate	D_{3d}
126.	VIJYES	$P1_12_1/n$	18-Crown-6 4-aminobenzosulfamide	D_{3d}
127.	VUXJUT	$P2_1/c$	1,4,7,10,13,16-Hexaoxacyclo-octadecane 2-isopropyl-3-methylphenol dihydrate	D_{3d}
128.	XIVMAQ	*P*-1	bis(Trimesic acid) 18-crown-6 dihydrate	D_{3d}
129.	XIVMAQ01	*P*-1	bis(benzene-1,3,5-tricarboxylic acid) 18-crown-6 dihydrate	D_{3d}
130.	XOWCOC	$P2_1/n$	Ammonia-(cyclotriborane) 18-crown-6	D_{3d}
131.	YALQOU	*Pbca*	2,5-difluorobenzene-1,3-diamine 18-crown-6	D_{3d}
132.	YEGVIP	*P*-1	18-Crown-6 dichloromethane solvate	D_{3d}
133.	YEGVIP01	*P*-1	18-crown-6 dichloromethane solvate	D_{3d}
134.	YIMZAV	$P2_1/n$	18-Crown-6 hexahydrate	D_{3d}
135.	YIMZAV01	$P2_1/n$	1,4,7,10,13,16-Hexaoxacyclooctadecane hexahydrate	D_{3d}
136.	YINFEG	$P2_1/n$	18-Crown-6 bis(di(benzenesulfonyl)amine) methanol solvate	D_{3d}
137.	YINFIK	*P*-1	18-Crown-6 bis(bis(4-chlorobenzenesulfonyl)amine) methanol solvate	D_{3d}
138.	YINFUW	$P2_1$	18-Crown-6 (benzenesulfonyl)(methanesulfonyl)amine methanol solvate	D_{3d}

139.	YIZCEP	*C*2/*c*	2,5,8,11,14,17-Hexaoxacyclo-octadecane bis(bis(benzenesulfonyl) amine) tetrahydrate	D_{3d}
140.	YIZCIT	$P2_1/c$	2,5,8,11,14,17-Hexaoxacyclo-octadecane bis(bis(4-fluorophenylsulfonyl)amine) dihydrate	D_{3d}
141.	YUSRAH	$P2_1/n$	bis(methanesulfonamide) 1,4,7,10,13,16-hexaoxacyclooctadecane	D_{3d}
142.	YUSREL	$P2_1/n$	bis(4-methylbenzenesulfonamide) 1,4,7,10,13,16-hexaoxacyclooctadecane	D_{3d}
143.	ZABRAV	$P1_12_1/n$	18-Crown-6 4-nitrosoaniline	D_{3d}
144.	ZIJQOY	*P*-1	(18-Crown-6) bis(1,2,4-1H-triazole)	D_{3d}
145.	ZIJQOY01	*P*-1	18-crown-6 bis(1H-1,2,4-triazole)	D_{3d}
146.	ZIJQOY02	*P*-1	18-crown-6 bis(1H-1,2,4-triazole)	D_{3d}
147.	ZOBBEX	$Pca2_1$	1,4,7,10,13,16-Hexaoxacyclotetradecane isonitrosocyanoacetamide monohydrate	D_{3d}
148.	ZORDEP	*P*-1	1,4,7,10,13,16-Hexaoxacyclo-octadecane bis(benzenesulfonyl)amine dihydrate ethanol solvate	D_{3d}
149.	FANSOG	*P*-1	bis(2-amino-4-chloro-3,5,6-trifluorobenzonitrile) 18-crown-6	C_i
150.	FANSUM	*P*-1	bis(2-amino-4-chloro-3,6-difluorobenzonitrile) 18-crown-6	C_i
151.	OGINIE	*P*-1	tris([1,2,5]thiadiazolo[3,4-c][1,2,5]thiadiazolo) 18-crown-6	C_i
152.	BAKHIE	*C*2/*c*	bis(2,4-Dinitroaniline) 1,4,7,10,13,16-hexaoxacyclo-octadecane clathrate	C_i
153.	BAPREQ	*P*-1	1,4,7,10,13,16-Hexaoxacyclooctadecane bis(1-((4-amino-1,2,5-thiadiazol-3-yl)carbonyl)thiosemicarbazide) clathrate	C_i
154.	BECVEK	$P2_1/c$	bis(4-Nitro-1,2-benzenediamine) 1,4,7,10,13,16-hexaoxacyclo-octadecane clathrate	C_i
155.	BODJOT	$P2_1/c$	1,4,7,10,13,16-Hexaoxacyclo-octadecane 4,4'-biphenyldiol dihydrate	C_i
156.	CEHGOL	$P2_1/c$	18-Crown-6 bis(dithio-oxamide)	C_i
157.	CENJAG	$P2_1/n$	18-Crown-6 tetrakis(methyl-4-aminobenzoate) clathrate	C_i
158.	CRWNUR	$P2_1/c$	1,4,7,10,13,16-Hexaoxacyclo-octadecane pentakis(urea) clathrate	C_i

159.	CRWNUR10	$P2_1/c$	18-Crown-6 pentakis(urea) clathrate	C_i
160.	CRWNUR11	$P2_1/c$	18-crown-6 pentakis(urea) clathrate	C_i
161.	CRWNUR12	$P2_1/c$	18-crown-6 pentakis(urea) clathrate	C_i
162.	DAFGID	$P2_1/c$	2-trifluoromethyl-4,6-difluoro-1,3-phenylenediamine hemikis(18-crown-6)	C_i
163.	DAWYOP	$P2_1$	18-Crown-6 tetrakis(thiourea) clathrate	C_i
164.	DIRXOS	P-1	bis(Triphenylsilyl) ether 18-crown-6	C_i
165.	DIWMOL10	$C2/c$	1,4,7,10,13,16-Hexaoxacyclo-octadecane bis(N-(m-chlorophenyl)urea) clathrate	C_i
166.	EPAQIW	$P2_1/n$	2,4,5,6-Tetrafluorobenzene-1,3-diamine 1,4,7,10,13,16-hexaoxacyclooctadecane	C_i
167.	EWAYIN	$C2/c$	2,6-diamino-3,5-difluorobenzonitrile 18-crown-6	C_i
168.	EWAZIO	P-1	2,4-diamino-3,5-difluorobenzonitrile 18-crown-6	C_i
169.	FABWAK	P-1	bis([(ethylamino)boranyl]aminoborane) (18-crown-6)	C_i
170.	FORRIP	$P2_1/n$	18-crown-6 1-broylamido-borazine	C_i
171.	HOXBSA	$P2_1/a$	1,4,7,10,13,16-Hexaoxacyclo-octadecane bis(benzenesulfonamide)	C_i
172.	HOXOCD	$Pbca$	1,4,7,10,13,16-Hexaoxacyclo-octadecane	C_i
173.	HOXOCD02	$Pbca$	1,4,7,10,13,16-Hexaoxacyclo-octadecane	C_i
174.	HOXOCD03	$Pbca$	1,4,7,10,13,16-Hexaoxacyclo-octadecane	C_i
175.	HUMTUE	$C2/c$	Tri-t-butylsilanol hemikis(18-crown-6) monohydrate	C_i
176.	HUQYAV	$P2_1/c$	18-Crown-6 bis(benzenesulfonamide)	C_i
177.	IKAXAT	$P2_1/c$	1,4,7,10,13,16-Hexaoxacyclo-octadecane bis(2-phenylhydrazinecarbothioamide) clathrate	C_i
178.	KIVKAB	$P2_1/c$	1,4,7,10,13,16-Hexa-oxacyclo-octadecane N-m-bromophenylurea clathrate	C_i
179.	OQIVUH01	P-1	(18-Crown-6) bis(1-methylthiourea) bis(1,2,3,4-tetrafluoro-5,6-diiodobenzene)	C_i

180.	SOVXUZ	*C*2/*c*	bis(3,5-dichloro-2,6-difluoropyridin-4-amine) 18-crown-6	C_i
181.	YALREL	$P2_1/n$	4,6-dichloro-2,5-difluorobenzene-1,3-diamine 18-crown-6	C_i
182.	YALRIP	$P2_1/n$	2,4,6-trichloro-5-fluorobenzene-1,3-diamine 18-crown-6	C_i
183.	ZAJKOK	*P*-1	18-Crown-6 bis(bis(2-naphthylsulfonyl)amine)	C_i
184.	ZAJKUQ	*P*-1	18-Crown-6 bis(bis(phenylsulfonyl)amine) isopropanol solvate	C_i
185.	AJUXUY	$P2_1/c$	18-Crown-6 dithiobiurea clathrate	C_2
186.	DUJPED	$P2_1/c$	18-Crown-6 bis(phosphoric acid) hexahydrate	C_{2h}
187.	EWAYEJ	$P2_1/c$	bis(2,4-diamino-3,5,6-trifluorobenzonitrile) 18-crown-6	C_{2h}
188.	JUNFON	*P*-1	18-Crown-6 bis(chloroacetonitrile) clathrate	C_{2h}
189.	LACKAB	*P*-1	18-Crown-6 bis(2,4-dinitroanisole) clathrate	C_{2h}
190.	NURJEP	$P2_1/n$	1,4,7,10,13,16-Hexaoxacyclo-octadecane bis(acetic acid) tetrahydrate	C_{2h}
191.	PUNXOO	*C*2/*m*	bis(4-amino-2,3,5,6-tetrafluorobenzoic acid) 18-crown-6	C_{2h}
192.	VICFOC	*P*-1	18-Crown-6 tetrakis(2-hydroxymethyl-4-(1,1,3,3-tetramethylbutyl)phenol) clathrate	C_{2h}
193.	XIVLOD	*P*-1	hexakis(5-Hydroxyisophthalic acid) 18-crown-6 clathrate decahydrate	C_{2h}
194.	XIVLOD01	*P*-1	hexakis(5-Hydroxyisophthalic acid) 18-crown-6 clathrate decahydrate	C_{2h}
195.	XIVLOD02	*P*-1	hexakis(5-Hydroxyisophthalic acid) 18-crown-6 clathrate decahydrate	C_{2h}
196.	YORRIG	$P1_12_1/a$	18-Crown-6 trans-tetrafluoro-diaqua-silicon dihydrate	C_{2h}
197.	YORRIG01	$P2_1/n$	18-Crown-6 trans-tetrafluoro-diaqua-silicon dihydrate	C_{2h}
198.	CATCEG	$P2_1/n$	1,4,7,10,13,16-Hexaoxacyclo-octadecane pyrimidine-2,4(1H,3H)-dithione monohydrate	C_1
199.	DUVROC	C2/c	1,3,5-tris(2,6-Dimethyl-4-hydroxyphenyl)benzene 18-crown-6 methanol monohydrate clathrate	C_1
200.	QUHYID	$P2_1/n$	dicyano-difluoro-selenium 18-crown-6	C_1

201.	VITWIE	$P1_12_1/a$	18-Crown-6 6-chloro-7-sulfamido-3,4-dihydro-1,2,4-benzothiadiazine-1,1-dioxide clathrate	C_1
202.	YIWKOE	P-1	Phenylalanine 3,5-bis(trifluoromethyl)phenylboronic acid 18-crown-6	C_1
203.	CEHGIF	P-1	18-Crown-6 N-methylthiourea	C_i, D_{3d}
204.	EWAYOT	P-1	2,6-diamino-4-chloro-3,5-difluorobenzonitrile 18-crown-6	C_i, D_{3d}
205.	LARVUY	P-1	bis(1H-imidazole-4,5-dicarbonitrile) 18-crown-6	C_i, D_{3d}
206.	LARVUY01	P-1	bis(1H-imidazole-4,5-dicarbonitrile) 18-crown-6	C_i, D_{3d}
207.	LARVUY02	P-1	bis(1H-imidazole-4,5-dicarbonitrile) 18-crown-6	C_i, D_{3d}
208.	OGIMOJ	$P2_1/n$	1,2,5-selenadiazole-3,4-dicarbonitrile 18-crown-6	C_i, D_{3d}
209.	OQIWOC	P-1	(18-Crown-6) 1-methylthiourea bis(1,2,4,5-tetrafluoro-3,6-dibromobenzene)	C_i, D_{3d}
210.	PEGXIK	P-1	1,4,7,10,13,16-hexaoxacyclooctadecane 3,5-dichloro-6-fluoropyridine-2,4-diamine	C_i, D_{3d}
211.	QUHYAV	$P2_1/n$	dicyano-selenium sesquikis(18-crown-6)	C_i, D_{3d}
212.	RIJVOV	P-1	bis(5-Amino-1H-tetrazole) 18-crown-6	C_i, D_{3d}
213.	YAKRIO	P-1	18-crown-6 2,4,6-trifluoro-1,3-phenylenediamine	C_i, D_{3d}
214.	YALRAH	P-1	4-chloro-2,5,6-trifluorobenzene-1,3-diamine 18-crown-6	C_i, D_{3d}

Table 4.2: Summary of various conformations of DCH18C6 with neutral molecules obtained from CSD database.

No:	*Refcode*	*Space Gp.*	**Dicyclohexano 18-crown-6; No errors; No ions; No disorders; only Organic; Hits- 39** *Compound Name (L)*	*Confor-mations*
1.	AJUXOS	$P2_1/n$	cis-anti-cis-Dicyclohexyl-18-crown-6 bis(dithiooxamine) clathrate	C_i
2.	CATCIK	$P2_1/n$	cis,anti,cis-(2,3:11,12-Dicyclohexano-1,4,7,10,13,16-hexaoxacyclo-octadecane) bis(pyrimidine-2,4(1H,3H)-dithione) clathrate	C_i
3.	DCHXCS01	$P2_1/n$	cis-anti-cis-Dicyclohexano-18-crown-6	C_i
4.	DCHXCS02	*Pccn*	cis-transoid-cis 2,5,8,15,18,21-hexaoxatricyclo(20.4.0.0$9,14!)hexacosane	C_i
5.	DCHXCT	*P*-1	trans-syn-trans-2,5,8,15,18,21-Hexaoxatricyclo(20.4.0.0$9,14!)hexacosane	C_i
6.	DCHXCT01	*P*-1	trans-syn-trans-2,5,8,15,18,21-Hexaoxatricyclo(20.4.0.0$9,14!)-hexacosane	C_i
7.	FUPLOR	*P*-1	cis-anti-cis-Dicyclohexyl-18-crown-6 bis(malononitrile)	C_i
8.	GEJDEG	$P2_1/c$	cis-anti-cis-Dicyclohexano-18-crown-6 bis(4-aminobenzoic acid) clathrate	C_i
9.	JEMVIG	*P*-1	cis-anti-cis-Dicyclohexano-18-crown-6 bis(4-aminobenzenesulfamide) clathrate	C_i
10.	JIFFUZ	$P2_1/n$	cis-anti-cis-Dicyclohexano-18-crown-6 bis(4-aminobenzenesulfamidine) clathrate	C_i
11.	KOGSEE	*P*-1	Dicyclohexane-18-crown-6 4-amino-3,5-dichlorobenzenesulfamide clathrate	C_i
12.	LACDIC	$P1_12_1/n$	cis-anti-cis-Dicyclohexano-18-crown-6 bis(2-methylbenzenesulfamide)	C_i
13.	LOFDAL	$P2_1/n$	cis,anti,cis-Dicyclohexano-18-crown-6 bis(2-thiouracil)	C_i

14.	NEWPEL	*Pccn*	cis-anti-cis-2,3;11,12-Dicyclohexano-1,4,7,10,13,16-hexaoxacyclo-octadecane bis(3-thioamidopyridine) monohydrate	C_i
15.	NIYGAD	$P2_1/n$	Dicyclohexano-18-crown-6 bis(monoaquatrifluoroboron)	C_i
16.	REZXEZ	*P*-1	cis-anti-cis-Dicyclohexano-18-crown-6 6-chloro-7-sulfamido-3,4-dihydro-1,2,4-benzothiadiazine-1,1-dioxide acetone solvate clathrate	C_i
17.	SEHDAL	*P*-1	2,5,8,15,18,21-Hexaoxa-tricyclo(20.4.0.0$9,14!)hexacosane bis(4-acetylaminobenzaldehyde thiosemicarbazone) bis(methanol) clathrate	C_i
18.	SISZID	*P*-1	cis-anti-cis-Dicyclohexano-18-crown-6 bis(maleic anhydride) clathrate	C_i
19.	TONFOR	*C*2/*c*	cis-anti-cis-Dicyclohexano-18-crown-6 3,4-diaminofurazane clathrate	C_i
20.	VEKKUR	$Pna2_1$	(cis-anti-cis-Dicyclohexano-18-crown-6) amidosulfuric acid clathrate	C_i
21.	VEVYIE	*P*-1	cis-anti-cis-Dicyclohexano-18-crown-6 bis(4-methylbenzenesulfamide) clathrate	C_i
22.	VOHVIX	$P1_12_1/b$	Dicyclohexano-18-crown-6 bis(4-acetylaminobenzenesulfonamide) clathrate	C_i
23.	VUGTUO	*P*-1	cis-anti-cis-2,5,8,15,18,21-hexaoxatricyclo[20.4.0.0$9,14!]hexacosane acetonitrile solvate	C_i
24.	WEJWOX	*P*-1	cis-anti-cis-Dicyclohexano-18-crown-6 bis(p-nitrobenzene sulfonamide) clathrate	C_i
25.	XAPVOZ	*P*-1	cis-anti-cis-Dicyclohexano-18-crown-6 bis(succinonitrile) clathrate	C_i
26.	ZABREZ	*Pbca*	Dicyclohexano-18-crown-6 bis(4-nitrosoaniline)	C_i
27.	ZUVYAQ	$P2_1/n$	2,5,8,15,18,21-Hexaoxatricyclo(20.4.0$1,22!.0$9,14!)hexacosane bis(monothioacetic acid)	C_i
28.	DCHXCR01	$P2_12_12_1$	cis-syn-cis-2,5,8,15,18,21-Hexaoxatricyclo(20.4.0.0$9,14!)hexacosane	C_2
29.	DCHXCR02	$P2_12_12_1$	icosahydrodibenzo[b,k][1,4,7,10,13,16]hexaoxacyclooctadecine	C_2
30.	AJUYAF	*Pn*	cis-anti-cis-Dicyclohexyl-18-crown-6 dithiobiurea clathrate	C_1

31.	CATCOQ	$P2_1/n$	cis,syn,cis-(2,3:11,12-Dicyclohexano-1,4,7,10,13,16-hexaoxacyclo-octadecane) pyrimidine-2,4(1H,3H)-dithione monohydrate	C_1
32.	MEBYID01	$P2_12_12_1$	cis-syn-cis-Dicyclohexano-18-crown-6 bis(4-aminobenzoic acid) clathrate	C_1
33.	JAPGAJ	*P*-1	cis-transoid-cis-5,8,11,16,19,22-Hexaoxaperhydrodibenzo(a,j)cyclo-octadecene 6-chloro-4-nitroso-3,4-dihydro-2H-1,2,4-benzothiadiazine-7-sulfonamide 1,1-dioxide clathrate	C_i, C_1, C_i
34.	FINQID	*P*-1	(cis-anti-cis)-(dicyclohexyl-18-crown-6) bis(N,N'-diphenylthiourea) clathrate	C_i, C_i
35.	FUPLIL	*Pbca*	cis-syn-cis-Dicyclohexyl-18-crown-6 malononitrile	C_s
36.	JIFFOT	*P*-1	cis-syn-cis-Dicyclohexano-18-crown-6 bis(4-aminobenzenesulfamidine) monohydrate clathrate	C_s
37.	KOGSEF	$A1_1a$	cis-syn-cis-Dicyclohexano-18-crown-6 3,5-dichloro-4-aminobenzenesulfamide clathrate	C_s
38.	VEKKOL	$P1_12_1/n$	(cis-syn-cis-Dicyclohexano-18-crown-6) amidosulfuric acid clathrate methanol solvate	C_s
39.	XAPVUF	*Pbca*	cis-anti-cis-Dicyclohexano-18-crown-6 glutaronitrile clathrate	C_s

Table 4.3: Summary of various conformations of B18C6 with neutral molecules obtained from CSD database.

No:	*Refcode*	*Space Gp.*	**B18C6 COCRYSTAL, No errors;No ions; No disorders; only Organic; Hits-11** *Compound Name (L)*	*Conformations*
1.	CATCUW	$P2_12_12_1$	2,3-Benzo-1,4,7,10,13,16-hexaoxacyclo-octadeca-2-ene pyrimidine-2,4(1H,3H)-dithione monohydrate	C_1
2.	CIPHAL	*P*-1	Nicotinamide benzo-[18]crown-6	C_1
3.	FOHMOG	*P*-1	4,4'-bi-1,3-thiazole-2,2'-diamine 2,3,5,6,8,9,11,12,14,15-decahydro-1,4,7,10,13,16-benzohexaoxacyclooctadecine methanol solvate	C_1
4.	FUFMID	$P2_1$	Thiourea benzo-[18]crown-6	C_1
5.	FUFMUP	$P2_1/n$	1-Methylthiourea benzo-[18]crown-6	C_1
6.	KEZZEU	$P2_1/n$	Benzo-18-crown-6 bis(methylsulfonyl)amine clathrate	C_1
7.	NEWPOV	*P*-1	2,3-Benzo-1,4,7,10,13,16-hexaoxacyclo-octadeca-2-ene 3-thioamidopyridine clathrate	C_1
8.	OQIJEF	*P*1	2,3,5,6,8,9,11,12,14,15-decahydro-1,4,7,10,13,16-benzohexaoxacyclooctadecine bis(1,2,3,4,5-pentafluoro-6-iodobenzene) thiourea	C_1
9.	OQIJIJ	$P2_1/n$	2,3,5,6,8,9,11,12,14,15-decahydro-1,4,7,10,13,16-benzohexaoxacyclooctadecine 1,2,4,5-tetrafluoro-3,6-diiodobenzene thiourea	C_1
10.	OQIJUV	*P2/c*	2,3,5,6,8,9,11,12,14,15-decahydro-1,4,7,10,13,16-benzohexaoxacyclooctadecine bis(1,2,4,5-tetrafluoro-3,6-diiodobenzene) bis(1-methylthiourea)	C_2
11.	SOVJIW	$P2_12_12_1$	Benzo-18-crown-6 aminosulfuric acid clathrate	C_2

Table 4.4: Summary of various conformations of DB18C6 with neutral molecules obtained from CSD database.

No:	***Refcode***	***Space Gp.***	DB18C6 COCRYSTAL; No errors; No ions; No disorders; only Organic; Hits- 11 ***Compound Name (L)***	***Conformations***
1.	ROFYIV	*Cc*	6,7,9,10,17,18,20,21-Octahydrodibenzo(b,k)(1,4,7,10,13,16)hexaoxacyclooctadecene	C_2
2.	ROFYIV01	*Cc*	6,7,9,10,17,18,20,21-octahydrodibenzo[b,k][1,4,7,10,13,16]hexaoxacyclooctadecine	C_2
3.	OGINAW	*C*2/*c*	[1,2,5]thiadiazolo[3,4-c][1,2,5]thiadiazolo dibenzo-18-crown-6 dichloromethane solvate	C_{2v}
4.	FEHYUM	$P2_1/c$	Dibenzo-18-crown-6 bis(nitromethane) clathrate	C_{2v}
5.	FEHYUM10	$P2_1/c$	Dibenzo-18-crown-6 bis(nitromethane) clathrate	C_{2v}
6.	FEHZAT	*P*-1	Dibenzo-18-crown-6 bis(acetonitrile) clathrate	C_{2v}
7.	FEHZAT10	*P*-1	Dibenzo-18-crown-6 bis(acetonitrile) clathrate	C_{2v}
8.	KODYIM	$Pna2_1$	Dibenzo-18-crown-6 bis(picric acid) trihydrate	C_{2v}
9.	OGINEA	*Cc*	1,2,5-selenadiazole-3,4-dicarbonitrile dibenzo-18-crown-6 dichloromethane solvate	C_{2v}
10.	XIVSIE	$P2_1/n$	Dibenzo-18-crown-6 2-methyl-p-nitroaniline	C_{2v}
11.	ZUVXUJ	$P2_1/c$	2,5,8,15,18,21-Hexaoxatricyclo(20.4.0$1,22!.0$9,14!)hexacosa-1(22),9,11,13,23,25-hexaene monothioacetic acid acetonitrile solvate	C_{2v}